

A Comparative Study of Sustainable Aviation Fuel Production from Hydroprocessing
Process Between Hydrogen Recovery Unit from Steam Reforming and Hydrogen
Generation Unit from Biomass Gasification



A Thesis Submitted in Partial Fulfillment of the Requirements
for the Degree of Master of Engineering in Chemical Engineering
Department of Chemical Engineering
Faculty Of Engineering
Chulalongkorn University
Academic Year 2023

การเปรียบเทียบกระบวนการผลิตเชื้อเพลิงอากาศยานชีวภาพโดยกระบวนการไฮโดรโปรเซสซึ่ง
ระหว่างการใช้หน่วยกักเก็บไฮโดรเจนโดยวิธีรีฟอร์มมิงด้วยไอน้ำและหน่วยผลิตก๊าซไฮโดรเจนจากแก๊ส

ซีพีเคชั่นชีวมวล



วิทยานิพนธ์นี้เป็นส่วนหนึ่งของการศึกษาตามหลักสูตรปริญญาวิศวกรรมศาสตรมหาบัณฑิต

สาขาวิชาวิศวกรรมเคมี ภาควิชาวิศวกรรมเคมี

คณะวิศวกรรมศาสตร์ จุฬาลงกรณ์มหาวิทยาลัย

ปีการศึกษา 2566

Thesis Title	A Comparative Study of Sustainable Aviation Fuel Production from Hydroprocessing Process Between Hydrogen Recovery Unit from Steam Reforming and Hydrogen Generation Unit from Biomass Gasification
By	Miss Praeva Pongsripipat
Field of Study	Chemical Engineering
Thesis Advisor	Professor SUTTICHAJ ASSABUMRUNGRAT, Ph.D.
Thesis Co Advisor	Assistant Professor Watcharapong Khodee, D.Eng.

Accepted by the FACULTY OF ENGINEERING, Chulalongkorn University in
Partial Fulfillment of the Requirement for the Master of Engineering

----- Dean of the FACULTY OF
ENGINEERING
(Professor SUPOT TEACHAVORASINSKUN, Ph.D.)

THESIS COMMITTEE

----- Chairman
(MERIKA CHANTHANUMATAPORN, Ph.D.)
----- Thesis Advisor
(Professor SUTTICHAJ ASSABUMRUNGRAT, Ph.D.)
----- Thesis Co-Advisor
(Assistant Professor Watcharapong Khodee, D.Eng.)
----- Examiner
(Professor ANONGNAT SOMWANGTHANAROJ, Ph.D.)
----- External Examiner
(Assistant Professor Weerawun Weerachapichasgul,
D.Eng.)

แพรวา พงษ์ศรีพิพัฒน์ : การเปรียบเทียบกระบวนการผลิตเชื้อเพลิงอากาศยานชีวภาพ โดยกระบวนการไฮโดรโปรเซสซิงระหว่างการใช้หน่วยกู้คืนไฮโดรเจนโดยวิธีรีฟอร์มมิง ด้วยไอน้ำและหน่วยผลิตก๊าซไฮโดรเจนจากแก๊สซิฟิเคชันชีวมวล. (A Comparative Study of Sustainable Aviation Fuel Production from Hydroprocessing Process Between Hydrogen Recovery Unit from Steam Reforming and Hydrogen Generation Unit from Biomass Gasification) อ.ที่ปรึกษาหลัก : ศ. ดร. สุทธิชัย อัสนะบำรุงรัตน์, อ.ที่ปรึกษาร่วม : ผศ. ดร.วัชรพงษ์ ขาวดี

น้ำมันอากาศยานเชื้อเพลิงชีวภาพสามารถผลิตได้จากหลายกระบวนการผลิต กระบวนการหนึ่งที่มีความนิยม คือ กระบวนการ Hydrotreating of esters and fatty acids (HEFA) อย่างไรก็ตาม กระบวนการผลิตวิธีนี้จำเป็นต้องใช้ปริมาณไฮโดรเจนสูงสำหรับทำปฏิกิริยาไฮโดรโปรเซสซิง เนื่องจากไฮโดรเจนถือว่ามีราคาที่สูง ทำให้มีผลกระทบในด้านเศรษฐศาสตร์การลงทุนสำหรับการผลิตน้ำมันอากาศยานเชื้อเพลิงชีวภาพ งานวิจัยนี้จึงมุ่งพัฒนากระบวนการผลิตน้ำมันอากาศยานเชื้อเพลิงชีวภาพโดยใช้โปรแกรม Aspen Plus ในการออกแบบกระบวนการผลิต โดยพิจารณา 2 กระบวนการผลิตเพื่อนำมาเปรียบเทียบ กระบวนการผลิตแบบที่ 1 เป็นกระบวนการผลิตน้ำมันเชื้อเพลิงอากาศยานชีวภาพโดยมีระบบกู้คืนไฮโดรเจนจากการใช้วิธีเปลี่ยนแปลงโครงสร้างโมเลกุลด้วยไอน้ำของผลิตภัณฑ์พลอยได้ของกระบวนการ ส่วนกระบวนการผลิตแบบที่ 2 เป็นกระบวนการผลิตน้ำมันเชื้อเพลิงอากาศยานชีวภาพโดยมีกระบวนการผลิตไฮโดรเจนจากการแปรรูปชีวมวล ผลลัพธ์ที่ได้พบว่า กระบวนการผลิตแบบที่ 2 มีประสิทธิภาพสูงกว่ากระบวนการผลิตแบบที่ 1 ทั้งในด้านประสิทธิภาพของกระบวนการผลิตและด้านเศรษฐศาสตร์การลงทุน เนื่องจากได้ผลผลิตร้อยละสูงกว่า จึงมียอดรายได้ที่สูงกว่า ส่งผลให้ระยะคืนทุนสั้นกว่า จึงเหมาะกับการลงทุนมากกว่า

สาขาวิชา วิศวกรรมเคมี

ปีการศึกษา 2566

ลายมือชื่อนิสิต

ลายมือชื่อ อ.ที่ปรึกษาหลัก

ลายมือชื่อ อ.ที่ปรึกษาร่วม

6570165021 : MAJOR CHEMICAL ENGINEERING

KEYWORD:

Praeva Pongsripipat : A Comparative Study of Sustainable Aviation Fuel Production from Hydroprocessing Process Between Hydrogen Recovery Unit from Steam Reforming and Hydrogen Generation Unit from Biomass Gasification. Advisor: Prof. SUTTICHAJ ASSABUMRUNGRAT, Ph.D. Co-advisor: Asst. Prof. Watcharapong Khodee, D.Eng.

Sustainable aviation fuel (SAF) can be generated using various processes. Among the well-established approaches, one that stands out is the hydrotreating of esters and fatty acids (HEFA). However, the HEFA process requires a source of hydrogen for the hydroprocessing reactions. Hydrogen is often considered as an expensive component, and its cost can have a significant impact on the overall economic viability of renewable aviation fuel production. In this work, the SAF process is developed using Aspen Plus simulation. There are 2 scenarios to be considered. Scenario 1 involves a plant in which the hydrotreating of palm oil is performed to recover hydrogen from the hydrocarbon gas and other byproducts directed to a steam reformer. In scenario 2, palm oil hydrotreatment is combined with hydrogen production through biomass gasification. The results show that scenario 2 is superior to the scenario 1 in both terms of performance and economics. This is attributed to its substantial SAF yield, resulting in higher revenue from product sales, as well as a shorter payback period.

Field of Study: Chemical Engineering

Academic Year: 2023

Student's Signature

Advisor's Signature

Co-advisor's Signature

ACKNOWLEDGEMENTS

I want to express my sincere appreciation to my thesis advisor, Prof. Suttichai Assabumrungrat, and co-advisor, Asst. Prof. Watcharapong Khodee, for their exceptional guidance and the conducive research environment they fostered. Their encouragement and insightful feedback inspired me to expand my research from various perspectives. I am immensely thankful for the time they dedicated to reviewing my thesis work.

I also extend my gratitude to my thesis chairman, Dr. Merika Chantanumataporn, and committee members Prof. Anongnat Somwangthanaroj and Asst. Prof. Weerawun Weerachapichasgul. Their valuable comments and suggestions significantly contributed to enhancing this work.

Finally, I deeply appreciate the consistent support, motivation, and understanding provided by my family, friends, and Mr.CS throughout my academic journey.

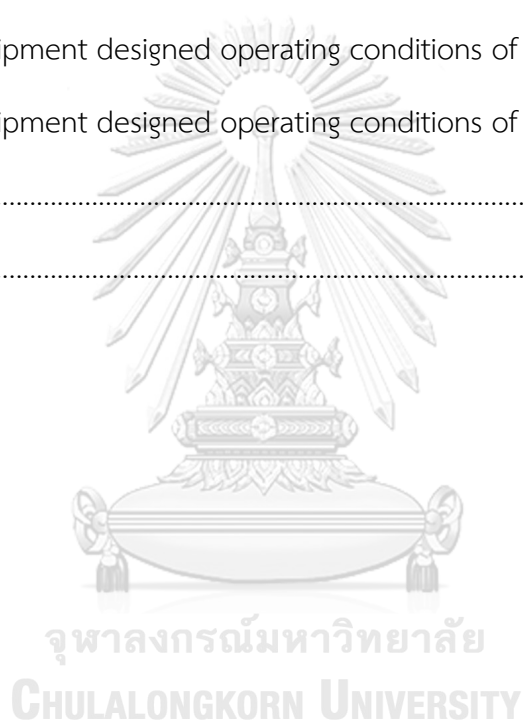
Praeva Pongsripipat

TABLE OF CONTENTS

	Page
ABSTRACT (THAI)	iii
ABSTRACT (ENGLISH)	iv
ACKNOWLEDGEMENTS	v
TABLE OF CONTENTS	vi
LIST OF TABLES.....	ix
LIST OF FIGURES.....	x
Chapter 1	1
Introduction.....	1
1.1 Background	1
1.2 Objectives of this research.....	2
1.3 Scopes of this research.....	2
1.4 Schedule plans	3
Chapter 2	4
Theory and literature reviews.....	4
2.1 Theory.....	4
2.1.1 Biojet fuel production	4
2.1.2 Hydrotreating of esters and fatty acids (HEFA).....	5
2.1.3 Biomass Gasification.....	8
2.2 Literature review.....	9
Chapter 3	18
Methodology.....	18

3.1 Defining Problem.....	19
3.2 Feedstock Potential.....	19
3.3 Conceptual Design.....	20
3.4 Process Simulation.....	21
3.5 Process Evaluation.....	22
3.5.1 Profitability Index (PI).....	22
3.5.2 Internal Rate of Return (IRR).....	22
3.5.3 Payback Period.....	23
3.5.4 Energy Utilization.....	23
3.5.5 Environmental Impact.....	23
Chapter 4.....	24
Results and Discussion.....	24
4.1 Model Validation.....	24
4.1.1 Thermodynamic Model Validation.....	24
4.1.2 SAF production with hydrogen recovery via steam reforming.....	25
4.1.3 SAF production with hydrogen generation via biomass gasification.....	29
4.1.4 Process optimization of biomass gasification unit.....	34
4.2 Comparison.....	35
4.2.1 Process Performance and Specific Energy Consumption.....	35
4.2.2 Process Economic Comparison.....	36
4.2.3 Environmental impact comparison.....	39
Chapter 5.....	40
Conclusions.....	40
5.1 Conclusions.....	40

Appendix	41
Appendix A Stream results of scenario 1	41
Appendix B Stream results of scenario 2	49
Appendix C Yield curve of experimental studies for the hydrogenation reactor [16]	55
Appendix D Yield curve of experimental studies for the hydrogenation reactor [16]	56
Appendix E Equipment designed operating conditions of scenario 1.	57
Appendix F Equipment designed operating conditions of scenario 2.	59
REFERENCES.....	61
VITA.....	64



LIST OF TABLES

	Page
Table 1 Gantt chart of schedule plans.	3
Table 2 Overview of the general production pathways to SAF.....	4
Table 3 Yield of liquid hydrocarbon products over different catalyst [15].	10
Table 4 Typical chemical compositions of palm kernel shell [18].	13
Table 5 Restricted chemical equilibrium in the GASI reactor [22].	15
Table 6 Triglycerides composition of several vegetable oils [9].....	25
Table 7 Comparing the mass balance of the HEFA process between Zoé Béalu study [16] and Scenario 1.....	27
Table 8 The mass balance of scenario 2.....	30
Table 9 Process Performance comparison between scenario 1 and scenario 2.....	35
Table 10 Total capital cost of the two scenarios.....	36
Table 11 Total operating cost of the two scenarios.....	37
Table 12 Process economics comparison between the two scenarios.....	38
Table 13 Environmental impact comparison between scenario 1 and scenario 2.....	39

LIST OF FIGURES

	Page
Figure 1 Reaction routes occurring during the hydrogenation of Triolein [10].	6
Figure 2 A diagram of gasifier showing different zones along with reactions [14].	9
Figure 3 Schematic diagram of the simulated process [16].	11
Figure 4 Comparison of simulation results from the kinetic models [20].	14
Figure 5 Aspen Plus flowsheet of biomass gasification model.	16
Figure 6 Overall methodology procedure.	18
Figure 7 Structure of triglyceride (Triolein)	19
Figure 8 Block flow diagram of scenario 1	21
Figure 9 Block flow diagram of scenario 2	21
Figure 10 The behavior of hydrogen gas and hexadecane (C ₁₆ H ₃₄) at 269 °C	25
Figure 11 The designed process diagram results of scenario 1	28
Figure 12 The designed process diagram results of scenario 2	31
Figure 13 Effect of gasification temperature on syngas composition	32
Figure 14 Effect of steam per biomass ratio on syngas composition	33

Chapter 1

Introduction

1.1 Background

The global community is currently grappling with major challenges, including the increasing energy demands driven by a growing population, the ongoing release of greenhouse gases from human activities, and the diminishing reserves of petroleum. In 2019, approximately 30% of the total energy consumed in the United States originated from the transportation sector, as reported by the Energy Information Agency (EIA) [1]. Within the realm of decarbonization efforts, the aviation sector has emerged as a critical focus area due to the greater complexity involved in making airplanes environmentally sustainable compared to regular vehicles. This is of paramount importance because aviation plays a vital role in facilitating efficient and speedy travel for both individuals and goods.

Among various modes of transportation, the aviation sector has witnessed the most significant expansion in the past decade. While this growth brings economic and societal advantages, it also exacerbates carbon dioxide emissions due to the extensive use of petroleum-derived kerosene in aviation, leading to substantial greenhouse gas emissions. In an effort to address this challenge, the International Air Transport Association (IATA) has committed to reducing CO₂ emissions from aviation by 50% by the year 2050 [2]. To achieve this goal, the adoption of renewable biojet fuels is imperative. Several processing techniques have received ASTM approval for producing renewable aviation fuel suitable for commercial passenger flights [3]. These techniques encompass alcohol to jet (ATJ), gas to jet (GTJ), sugars/platform molecules to jet (STJ), and oil to jet (OTJ) [4]. Among these approaches, hydroprocessed ester and fatty acids (HEFA) stand out as the most advanced method for producing sustainable aviation fuel (SAF).

The HEFA process entails the transformation of triglyceride feedstock into biojet fuel and renewable hydrocarbons through a sequence of procedures, including hydrodeoxygenation, hydroisomerization, and hydrocracking. These resultant products

are then separated using a distillation system. The hydrodeoxygenation (HDO) phase demands a substantial quantity of hydrogen, leading to increased expenses due to the requirement for significant volumes of hydrogen gas.

At present, most of the necessary hydrogen is generated through steam reforming, a method that emits greenhouse gases (GHGs), thus making the supply of hydrogen an important concern. To mitigate GHG emissions, the emphasis is on adopting green hydrogen production techniques. The primary objective of this research is to develop a process that can function without relying on external sources of hydrogen. This holistic approach has the potential to align with circular economy principles and enhance the efficiency of material management. Biomass gasification, a promising thermochemical method for generating green hydrogen from biomass sources like algae, sewage sludge, and agricultural crop waste, presents a viable solution. While biomass gasification has demonstrated its efficacy in hydrogen production, further investigation is warranted.

This study examines two distinct scenarios within a process plant to conduct a comparative analysis. In the first scenario, SAF byproduct is utilized in the process of its valorization through hydrogen production via steam reforming while the second scenario involves the integration of a biomass gasification plant for the production of green hydrogen.

1.2 Objectives of this research

1.2.1 To develop a process for producing sustainable aviation fuel from the hydroprocessing of crude palm oil with a plant that produces hydrogen via biomass gasification.

1.2.2 To provide an economic analysis of the process.

1.2.3 To provide a comparative study between hydrogen generation from the process byproduct via steam reforming and from biomass gasification.

1.3 Scopes of this research

1.3.1 The process model is simulated by Aspen Plus, and the economic analysis is evaluated by Aspen Economic Analysis.

Chapter 2

Theory and literature reviews

This chapter provides the related theory and literature review along with useful information for the research, including general information on the chemicals used, the field of biojet fuel production, and the past literature, which will help to simulate the process in this work.

2.1 Theory

2.1.1 Biojet fuel production

SAF referred to as biojet fuel, is a biomass-derived synthesized paraffinic kerosene (SPK) that is blended into conventionally petroleum-derived jet fuel [5]. Nevertheless, biojet fuel presents advantages such as higher energy density, decreased sulfur and oxygen levels, and a better freezing point compared to traditional jet fuel [6]. The production of SAF involves four primary biomass conversion methods as detailed in Table 2.

Table 2 Overview of the general production pathways to SAF

Conversion Pathway	Descriptions
Oil-to-SAF	Catalytic Deoxygenation of mono-, di-, and triglycerides, free fatty acids, and fatty acid esters, through hydroprocessing, followed by isomerization
Sugar-to-SAF	Hydrolysis to obtain fermentable syngas; sugars fermented to yield farnesene, followed by hydroprocessing and fermentation
Gas-to-SAF	Gasification to obtain syngas; Fischer-Tropsch (FT) to synthesize paraffin and olefins, followed by hydroprocessing
Alcohol-to-SAF	Hydrolysis to obtain fermentable sugars; sugars fermented to yield isobutanol and ethanol, followed by dehydration, oligomerization, hydrogenation, and fractionation

Oil to SAF, also recognized as the hydrotreating of esters and fatty acids (HEFA), represents one of the most well-established methods to create SAF. HEFA is a biojet fuel produced from vegetable oils and animal fats via hydroprocessing. This process entails a sequence of hydrogen-involved catalytic reactions. Within HEFA, two primary types of catalytic reactions are utilized to produce SAF [7]. In the initial set of reactions, the catalyst facilitates the elimination of oxygen from the oil feedstock, leading to the formation of linear hydrocarbons. The subsequent phase involves catalytic cracking and isomerization reactions, which generate hydrocarbons that are either shorter or possess branching. This step enhances the flow characteristics of the hydrocarbon mixture while simultaneously reducing its freezing point.

2.1.2 Hydrotreating of esters and fatty acids (HEFA)

Plant oil triglycerides, such as tripalmitin and triolein, can undergo a catalytic hydrotreating process. This process involves the conversion of unsaturated triglycerides into saturated ones through hydrogenation, followed by the cleavage of one triglyceride molecule into three fatty acid molecules through hydrogenolysis. Subsequently, these fatty acids can follow one of three distinct pathways: hydrodeoxygenation (HDO), decarbonylation (DCO), or decarboxylation (DCO₂), leading to the production of biojet fuel.

In the HDO pathway, a metal catalyst is employed to eliminate oxygen from the fatty acid molecule. The resulting product from this reaction consists of n-alkanes with the same carbon content as the corresponding fatty acids. DCO removes oxygen by releasing CO, while DCO₂ eliminates CO₂ from the free fatty acid molecules. As a result, the straight-chain alkane products generated will contain one fewer carbon atom than the original fatty acid [8], [9]. These three reactions play a pivotal role in removing oxygen from triglycerides and also influence the characteristics of the resulting hydrocarbon products. Figure 1 illustrates these three reactions using triolein as an example, as it is the primary component found in plant oils.

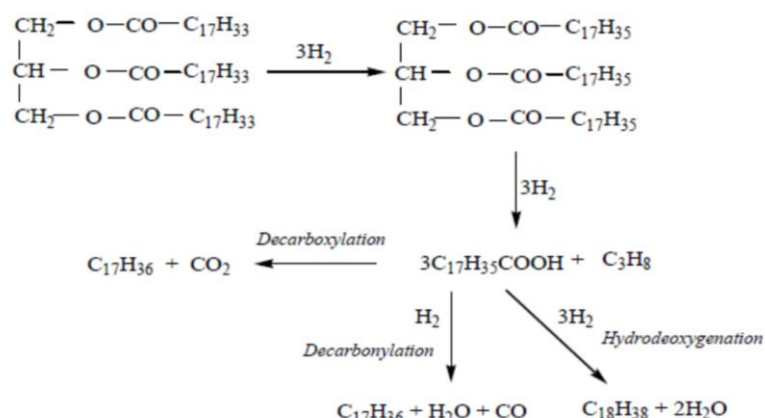


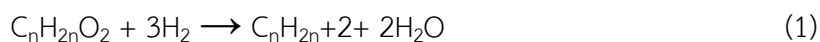
Figure 1 Reaction routes occurring during the hydrogenation of Triolein [10].

a) Hydrogenation and hydrogenolysis

Hydrogenation transforms unsaturated or double-bond triglycerides into saturated fatty acids. Reducing the level of unsaturation in the base oil is essential because it impacts the chemical stability and reactivity during the deoxygenation reaction, ultimately influencing the formation of various n-alkane products. From a chemical perspective, saturated fatty acids exhibit superior oxidative stability. Furthermore, the amount of hydrogen consumed in this process depends on the quantity of double bonds present in the base oil.

b) Hydrodeoxygenation (HDO)

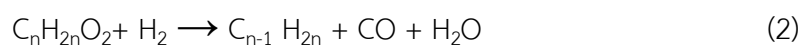
During the process of hydrodeoxygenation, the conversion of fatty acids results in the removal of oxygen, converting it into water (H_2O). This method offers the advantage of producing n-alkane products with the same number of carbon atoms as the original fatty acid, as depicted in equation (1).



c) Decarbonylation (DCO)

The process of eliminating a carbonyl group under high-pressure hydrogen conditions to produce an n-alkane product with one less carbon atom than the original fatty acid feed is termed decarbonylation (DCO). This reaction generates carbon monoxide (CO)

and water molecules as byproducts, as illustrated in equation (2). In the case of the DCO₂ reaction, formic acid acts as an intermediate, which can subsequently undergo decomposition to form n-alkane through dehydration, releasing both CO and H₂O.



d) Decarboxylation (DCO₂)

Decarboxylation (DCO₂) involves the removal of oxygen from the fatty acid chain by eliminating the carboxyl group in the form of carbon dioxide (CO₂), as illustrated in equation (3). Carboxylic acid and unsaturated glycerol di-fatty ester originate from triglycerides. Through hydrogenation, they are transformed to release fatty acid and produce n-alkane hydrocarbons, each with one less carbon atom than the original compound. The advantage of the DCO₂ pathway lies in the fact that it doesn't require hydrogen to convert a carboxylic acid into a normal paraffin and CO₂.



e) Cracking and isomerization

Hydrocracking of lengthy paraffin molecules is a common procedure in petroleum refineries. In this cracking reaction, high-boiling-point hydrocarbon components are converted into valuable fuels like gasoline and jet fuel, which typically consist of hydrocarbon chains ranging from C₉ to C₁₅. Conversely, isomerization, as depicted in equation (4), is a reaction that transforms straight-chain alkanes into their branched-chain counterparts. This process alters the arrangement of atoms in a molecule while maintaining the same constituent atoms. Consequently, both hydrocracking and isomerization can be employed to enhance the hydrodeoxygenation (HDO) process.



f) Separation of the products

Following the cracking and isomerization procedures, the blend of hydrocarbons undergoes a distillation step to divide them into diesel, jet fuel, and naphtha fractions. Before this, the gaseous byproducts, including excess hydrogen, carbon monoxide, carbon dioxide, propane, and remaining hydrocarbon gas, need to be separated and directed towards hydrogen recovery. In this context, another reaction that can take place is the water-gas-shift reaction, as illustrated in equation (7), which helps fulfill the internal hydrogen requirements.



2.1.3 Biomass Gasification

The concept of biomass encompasses a wide range of materials, including raw sources like wood, crops, and agricultural leftovers, as well as processed organic substances. The composition of biomass primarily consists of cellulose, hemicellulose, lignin, lipids, proteins, sugars, and starches, with specific components depending on whether the feedstock originates from plants or animals [11].

Biomass is characterized by a carbon dioxide (CO₂) cycle that is carbon-neutral, which means it does not release CO₂ into the environment during processing. This attribute has led to a growing emphasis on producing syngas from biomass rather than relying on fossil fuels. There are two primary methods for generating hydrogen from biomass: thermochemical and biochemical processes. Thermochemical processes, such as gasification, pyrolysis, and direct combustion, involve using biomass as a feedstock. Among these thermochemical processes, biomass gasification has garnered more attention due to its potential for polygeneration, which enables the production of additional products like heat, electricity, valuable chemicals, or biofuels alongside hydrogen [12].

Gasification belongs to the category of thermochemical processes, wherein carbon-rich materials like biomass are transformed into fuels or chemicals. The process of biomass gasification involves the utilization of various gasifying agents like air, steam, oxygen, or combinations thereof. It comprises four primary stages: drying, pyrolysis,

reduction, and oxidation [13]. A visual representation of this process can be seen in Figure 2, which illustrates a downdraft gasifier with distinct zones and associated reactions [14].

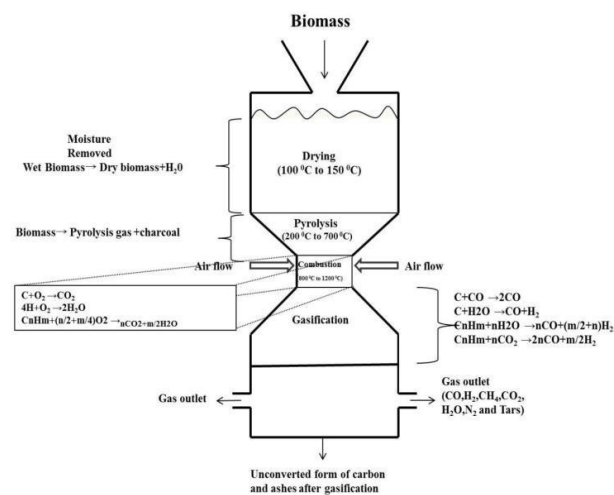


Figure 2 A diagram of gasifier showing different zones along with reactions [14].

The gasification process is subject to various factors that exert significant influence on the final outcomes. Factors such as the starting material, the agents used for gasification, operational conditions, the type of gasifier employed, and the presence of catalysts all impact the quantity and calorific value of the resulting gas product. Gasification conducted at lower temperatures may yield a product gas containing H_2 , CO , CO_2 , methane, and other impurities, whereas gasification carried out at higher temperatures produces synthetic gas, known as syngas. Syngas comprises H_2 , CO , CO_2 , water, light hydrocarbons, and fewer impurities compared to product gas [15]

2.2 Literature review

Gong et al. [15] examined the hydrotreatment of inedible jatropha oils using both PtPd/ Al_2O_3 catalysts and NiMoP/ Al_2O_3 catalysts. This investigation was carried out in a fixed-bed reactor under specific conditions: temperatures ranging from 330 to 390 °C,

a pressure of 3 MPa, and a flow rate of 2 h⁻¹. The key findings from this study can be summarized as follows: both the PtPd/Al₂O₃ catalyst and the two sulfided NiMoP/Al₂O₃ catalysts demonstrated strong performance. Table 3 provides data on the product yields and components of liquid hydrocarbons produced using different catalysts after a 5-hour reaction period. All catalysts achieved significantly higher yields (ranging from 81.2% to 83.9% by weight) of liquid hydrocarbon products, while the yields of gas hydrocarbons and water showed variations, ranging from 5.6% to 5.7% and from 4.3% to 7.6%, respectively.

By comparing the yields of liquid hydrocarbon products from these catalysts to theoretical values, it can be confidently concluded that nearly all the triglycerides in the jatropha oil were successfully converted into hydrocarbons. Additionally, it is evident that the PtPd/Al₂O₃ catalyst yielded lower amounts of water and total hydrocarbons compared to the other two NiMo catalysts. This difference can be attributed to the oxygen removal mechanism of the PtPd/Al₂O₃ catalyst, which primarily involves decarboxylation or decarbonylation, resulting in the formation of mainly CO and CO₂. In contrast, the other two NiMo catalysts primarily underwent hydrodeoxygenation, leading to the generation of a significant amount of water. The formation of CO and CO₂ also implies a loss of one carbon atom from the hydrocarbon products.

Table 3 Yield of liquid hydrocarbon products over different catalyst [15].

Catalyst	PtPd/ Al ₂ O ₃	NiMoP/Al ₂ O ₃
Liquid hydrocarbon yield (wt%)	81.2	83.9
Gas hydrocarbon yield (wt %)	5.6	5.6
Water yield (wt%)	4.3	7.5

Zoé Béalu. [16] studied the HEFA process using rapeseed oil as the feedstock. The work aimed to advance the production of alternative jet fuel in a manner that would achieve hydrogen self-sufficiency. This was accomplished by directing the remaining gas products to a steam reformer, thereby increasing the hydrogen supply to meet the

internal hydrogen requirements of the HEFA process. Figure 3 illustrates a simplified schematic of the entire process that was simulated in this research.

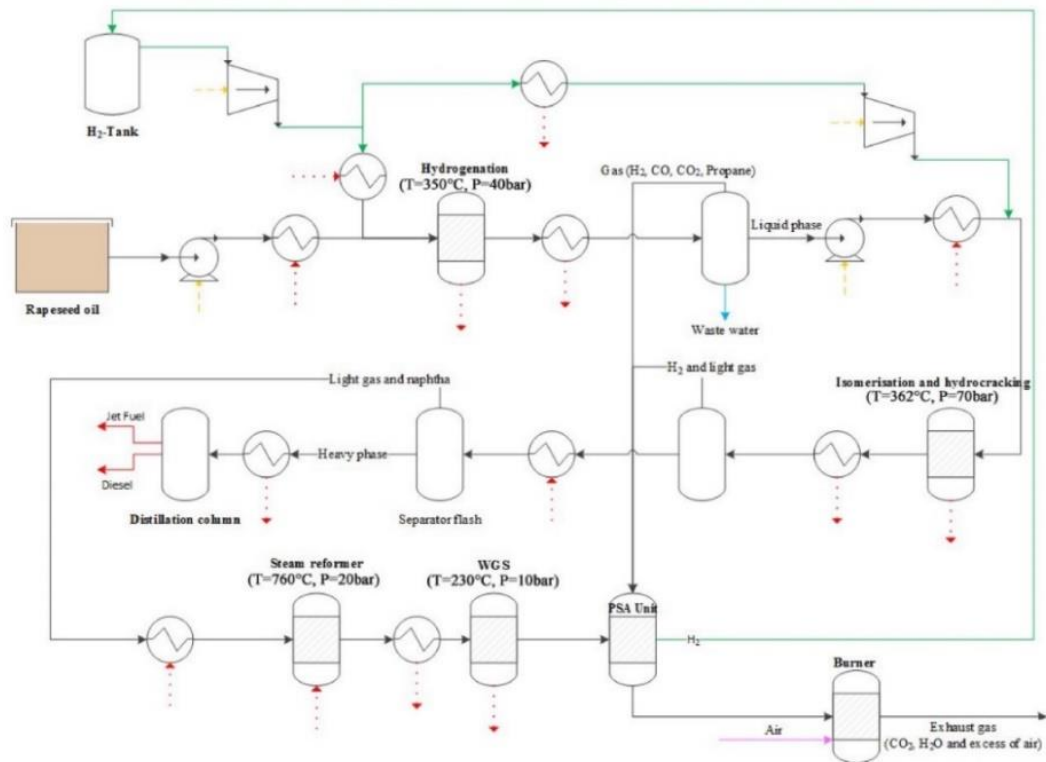


Figure 3 Schematic diagram of the simulated process [16].

The result of mass balance using Aspen Plus process simulation shows that throughput of 10,000 kg/h of rapeseed oil generates 7,710 kg/h of biojet fuel and 267 kg/h of diesel. Moreover, approximately 397 kg/h of hydrogen is necessary for the entire process involving 7,710 kg/h of crude palm oil, with the potential for recycling 397 kg/h of hydrogen from the gaseous output of the gas-liquid separator. Calculating based on the mass flow outcomes, the yield of SAF, represented as the ratio of produced SAF to the utilized rapeseed oil, stands at 77%. It thus shows that the process has good efficiency but the net production cost (NPC) of this process is high due to the feedstock price.

Farouk et al. [17] reported that produce significant quantities of biojet fuel through the HEFA process, reaching an output of 50,000 tonnes of biojet fuel annually would necessitate a supply of approximately 60,000 tonnes per year of high-quality vegetable

oil, properly filtered used cooking oil, or purified rendered animal fats. If the feedstock were crude palm oil, achieving this volume would require a yearly harvest from about 15,000 hectares of land. However, if jatropha oil were used, it would necessitate up to 50,000 hectares annually, and if rapeseed or soy oil were the feedstock, it would require up to 100,000 hectares per year. These commonly traded edible oils are currently priced at an international bulk rate of US\$900-1200 per tonne upon delivery, and these prices are showing an upward trend, closely following the fluctuation of crude oil prices.

According to **S.H. Pranolo et al. [18]**, the production of crude palm oil generates approximately 70% of solid waste materials during post-processing, including components like trunks, fronds, leaves, empty fruit bunches, and shells. Among these waste materials, shells are particularly noteworthy due to their high heating values (HHV), making them a highly promising source of biomass energy. In recent times, the majority of palm kernel shells (PKS) have been employed to fulfill the heat requirements of boilers in palm oil mills or biomass-based power plants through direct combustion. Beyond direct combustion, there is growing interest in gasifying PKS and other biomass materials. This approach is not only valuable for producing heat and power but also as a source of raw materials for the production of bio-based chemicals, including hydrogen.

Gasification provides an adaptable approach for transforming palm kernel shells into a gaseous fuel referred to as fuel gas or producer gas. The composition of this gas typically comprises H_2 , CO , and CH_4 , which can vary based on the composition of the feedstock [18]. The chemical composition traits and calorific value of palm kernel shells were evaluated using standard ASTM methods, and the results are presented in Table 4.

Table 4 Typical chemical compositions of palm kernel shell [18].

Parameter	Value (wt.%)	Method
Proximate Analysis (air-dried basis)		
Moisture Content	7.03	ASTM D.3173
Volatile Matter	71.24	ASTM D.3175
Fixed Carbon	19.57	ASTM D.3172
Ash	2.16	ASTM D.3174
Ultimate Analysis (dry ash free)		
C	48.35	ASTM D.5373
H	6.10	ASTM D.5373
N	0.48	ASTM D.5373
S	0.02	ASTM D.4239
O	42.88	ASTM D.3176

Furthermore, an assessment of the environmental effects resulting from the gasification of woody biomasses and forestry residues for power generation was conducted, focusing on global warming potential (GWP), acidification potential (AP), and eutrophication potential (EP). This analysis was carried out using a Life Cycle Analysis (LCA) methodology [18]. Within the cradle-to-gate scope of evaluation, the process was found to emit greenhouse gases (GHG) within the range of 43-62 kg CO₂-equivalents per ton of feedstock. The primary contributor to this emission is transportation, followed by feedstock pretreatment processes, while the combustion process itself has the smallest GHG impact, as biogenic CO₂ released is not considered a significant contributor to global warming.

The process also generated acidic gases, ranging from 23-74 kg SO₂-equivalents per ton of raw feedstock, with the combustion process during the second stage of conversion being the primary contributor to this impact. Additionally, this combustion process was identified as the main driver of the eutrophic effect, with values ranging from 97-247 kg NO₃-equivalents per ton of raw feedstock.

M. Puig-Gamero and colleagues [19] conducted simulations of the direct gasification process of biomass in a bubbling fluidized bed reactor, which involves the use of air. These models were fine-tuned and subsequently verified using a range of experimental data obtained from the gasification of four diverse biomass types in a pilot-scale bubbling fluidized bed reactor. The experiments covered various equivalence ratios ranging from 0.17 to 0.35 and temperatures from 709°C to 859°C.

The simulation results, which included the concentrations of CO, CO₂, H₂, CH₄, and C₂H₄ in the producer gas, closely matched the experimental data for various biomass types and operating conditions. This agreement is illustrated in Figure 4, which provides a comparison of the simulation results from kinetic models found in the literature by Champion et al. (2014) [20] and Martinez-Gonzalez et al. (2018) [21], alongside Model 1 proposed in M. Puig-Gamero's study. Among the gases analyzed, H₂ gas showed the lowest level of accuracy in predictions, consistently being overestimated. However, it's worth noting that the highest absolute error observed for H₂ was only 4.4%. Lastly, the predicted tar concentration ranged from 20 to 42 g/Nm³, decreasing as the equivalence ratio, temperature, and biomass particle size increased.

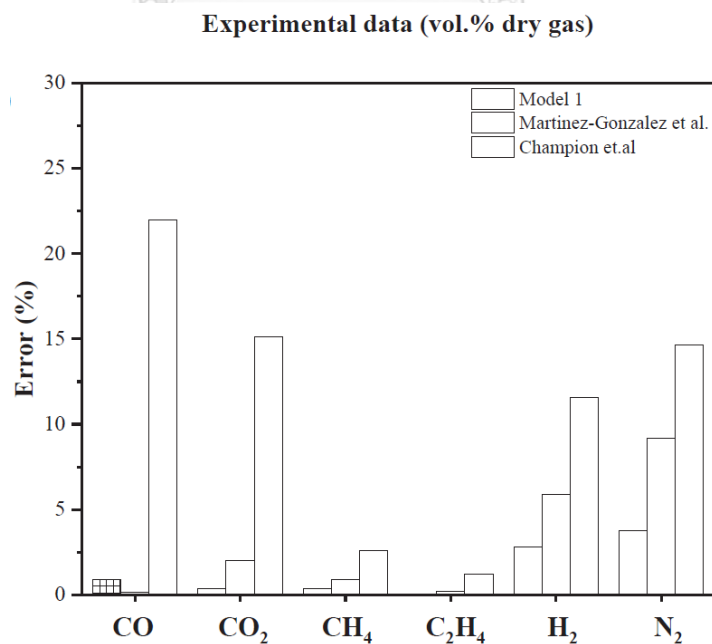


Figure 4 Comparison of simulation results from the kinetic models [20].

Saccara et al. [22] have conducted a comparative evaluation of various hydrogen production methods using renewable energy sources. Specifically, they examined polymer electrolyte membrane electrolysis, solid oxide electrolyze cell electrolysis, and biomass gasification using Aspen Plus V11. The researchers developed models and carried out simulations, focusing on sensitivity analyses to gain valuable insights into the behavior of these processes.

In biomass gasification, the Aspen Plus model's process flow diagram is depicted in Figure 5. The initial step involves the decomposition of biomass into its constituent chemical compounds (including hydrogen, carbon monoxide, carbon dioxide, oxygen, nitrogen, and sulfur) through the pyrolysis process, which takes place within the "PYRO" reactor. In the "CHAR-SEP" separator unit, the separation of solid (char) from the volatile portion occurs. Steam, which is a necessary component for gasification, is introduced into the "GASI" block at a temperature of 150°C and a pressure of 1 atm. The gasification process is carried out in the "GASI" reactor, with calculations based on Gibbs free energy minimization and utilizing restricted chemical equilibrium as the calculation option. The specific reactions involved are detailed in Table 5.

Table 5 Restricted chemical equilibrium in the GASI reactor [22].

Reaction Number	Reaction Scheme	Reaction Name	Heat of Reaction ΔH (kJ/mol)
1	$C + O_2 \rightarrow CO_2$	Carbon combustion	-393.0
2	$C + 0.5 O_2 \rightarrow CO$	Carbon partial oxidation	-112.0
3	$C + CO_2 \rightarrow 2 CO$	Boudouard reaction	+172.0
4	$C + H_2O \rightarrow CO + H_2$	Water gas shift reaction	+131.0
5	$CO + H_2O \rightarrow CO_2 + H_2$	Water gas shift reaction	-41.0
6	$C + 2 H_2 \rightarrow CH_4$	Methanation of carbon	-74.0
7	$H_2 + 0.5 O_2 \rightarrow H_2O$	Hydrogen partial combustion	-242.0
8	$CH_4 + H_2O \rightarrow CO + 3 H_2$	Steam reforming of methane	+206.0
9	$H_2 + S \rightarrow H_2S$	H ₂ S formation	-20.2

The gasification of char takes place in a plug flow reactor known as "CHAR-GAS," where kinetic reactions are incorporated. A power-law reaction kinetics model was employed, utilizing parameters as documented in [23]. The final step in biomass gasification involves syngas purification, which is crucial for eliminating water, ash, and

H₂S, resulting in a high hydrogen content syngas. In the simulation, this purification process is accomplished through a series of separation units. The model's validation was conducted using literature data, with a particular focus on data provided by [23].

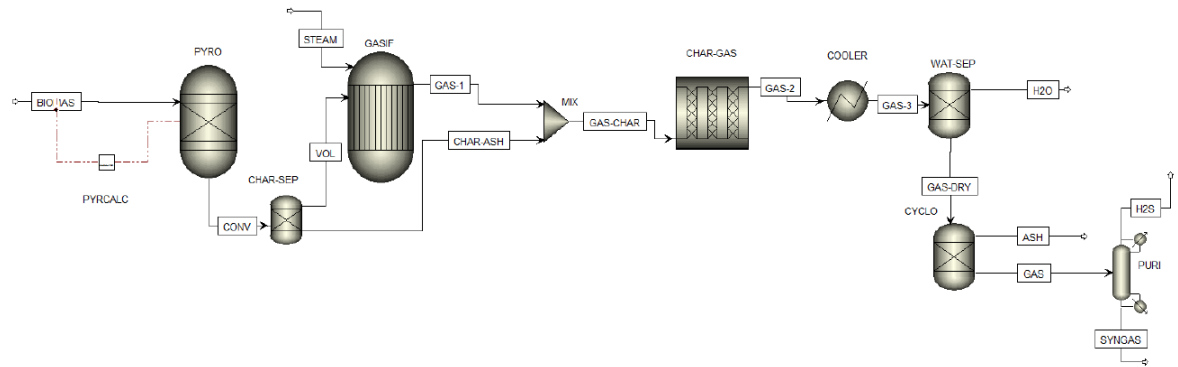


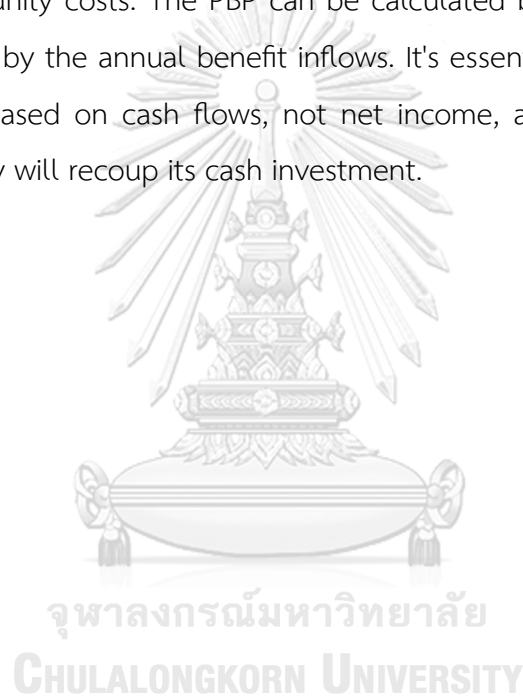
Figure 5 Aspen Plus flowsheet of biomass gasification model.

Hsu et al. [24] conducted a study involving process simulation and techno-economic analysis of the hydroprocessing of crude palm oil, focusing on a production capacity of 600 tonnes per day. The study estimated the production cost and calculated the minimum selling price of diesel while considering variations in material costs, plant capacity, operating conditions, and the use of different catalysts between Pd/C and NiMo/ γ -Al₂O₃.

The simulation was executed using the Aspen Plus program, employing the NRTL model. The raw materials underwent feeding and consecutive reactions in five reactors using RStioc, followed by distillation in a distillation column. The renewable diesel product was blended with the distillate from the first column. Through a techno-economic assessment, a proposed selling price of \$1.72 per liter was determined. Additionally, it was observed that increasing the plant capacity from 600 tonnes to 2,000 tonnes per day would result in a decrease in the selling price by 1 cent per liter. Moreover, the use of the NiMo/ γ -Al₂O₃ catalyst was found to contribute to a lower selling price compared to the Pd/C catalyst.

G. Reniers et al. [25] conducted a study on cost-benefit analysis as a tool for assessing safety measures and comparing various safety-related investments. Investment analysis provides a means to calculate the payback period (PBP), which is

a critical factor in determining whether to proceed with a safety project and invest in safety measures. The payback period (PBP) is defined as the time required, typically expressed in years, to recover an investment, thereby identifying the point at which the initial investment is repaid. The PBP of a safety investment plays a pivotal role in the decision-making process regarding safety projects, as longer PBPs are generally less favorable for some companies. It's important to note that PBP does not take into account any benefits that may occur beyond the determined time frame, nor does it gauge profitability. Additionally, it does not consider factors such as the time value of money or opportunity costs. The PBP can be calculated by dividing the cost of the safety investment by the annual benefit inflows. It's essential to emphasize that PBP calculations are based on cash flows, not net income, and solely determine how quickly a company will recoup its cash investment.



Chapter 3

Methodology

This chapter describes the steps and specifications involved in creating a simulation model for the production of SAF using crude palm oil. Additionally, it covers the process of assessing both the economic analysis and the environmental consequences. Figure 6 illustrates the overall methodology steps utilized in this research.

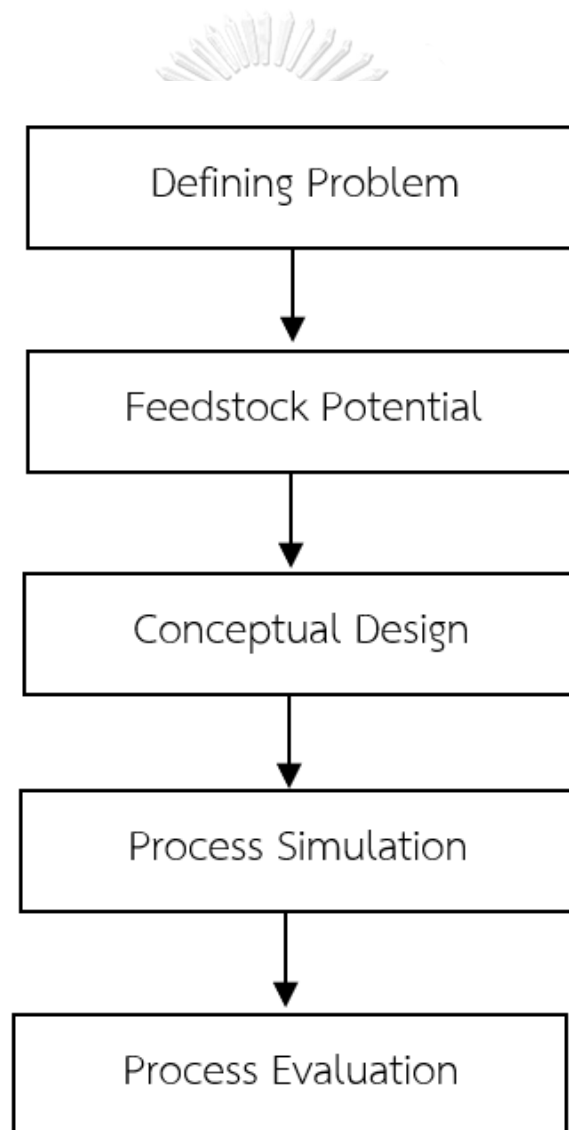


Figure 6 Overall methodology procedure.

3.1 Defining Problem

The primary objective of this study is to enhance the current biojet fuel production process by ensuring it becomes self-sufficient in hydrogen production. To address the economic constraints associated with the hydroprocessing plant, the plan is to utilize the same infrastructure as the existing facility, making necessary adjustments. This involves modifying the operating conditions to produce both desired products. The study also includes process optimization and the evaluation of various operational expenses.

3.2 Feedstock Potential

The HEFA process relies on triglycerides, which constitute the primary components of all natural vegetable oils and fats. A triglyceride molecule consists of glycerol and three fatty acids, as depicted in Figure 7. These fatty acids may be either saturated or unsaturated. The level of saturation in a triglyceride affects the hydrogenation process; the more saturated the molecule is, the lower the extent of hydrogenation required.

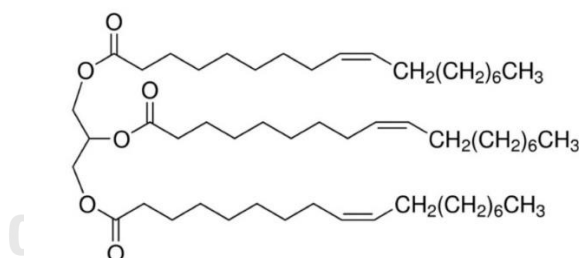


Figure 7 Structure of triglyceride (Triolein)

The selection of raw materials for the procedure offers a wide range of options, including various products containing oils and fats like vegetable oil, recycled cooking oil, and animal fats. In the context of this research, which concentrates on implementing the HEFA process in Thailand, it has been determined that palm oil demonstrates promising potential, with a sufficient yield of oil and fat for fuel production.

3.3 Conceptual Design

The production of sustainable aviation fuel (SAF) through the hydrotreating of esters and fatty acids (HEFA) is among the most established techniques. This process involves a series of catalytic reactions that rely on hydrogen. HEFA employs two main types of catalytic reactions to produce SAF [28, 29]. In the initial reactions, the catalyst aids in removing oxygen from the oil feedstock, resulting in the creation of linear hydrocarbons. The subsequent phase encompasses catalytic cracking and isomerization reactions, generating hydrocarbons that are either shorter or exhibit branching. This step enhances the flow properties of the hydrocarbon mixture while simultaneously lowering its freezing point. The present investigation evaluates the economic and environmental impacts of combining catalytic deoxygenation with hydrogen generation via biomass gasification for SAF production. This objective is pursued through the examination of two separate scenarios.

Scenario 1 (SAF production with hydrogen generation via steam reforming of the byproduct of the process): Figure 8 shows a simplified block flow diagram for the entire process of scenario 1. This scenario involves the production of SAF using a hydrogen recovery unit. The primary process steps encompass hydrogenation and hydrodeoxygenation of crude palm oil, followed by the isomerization and hydrocracking of the resultant deoxygenated products. Ultimately, a distillation column is employed to segregate the products, yielding the intended jet fuel and diesel. For the gaseous output, which comprises hydrogen, carbon dioxide, and residual hydrocarbon gas, a preliminary separation process is imperative. This separation facilitates hydrogen recovery, addressing the internal hydrogen requirement.

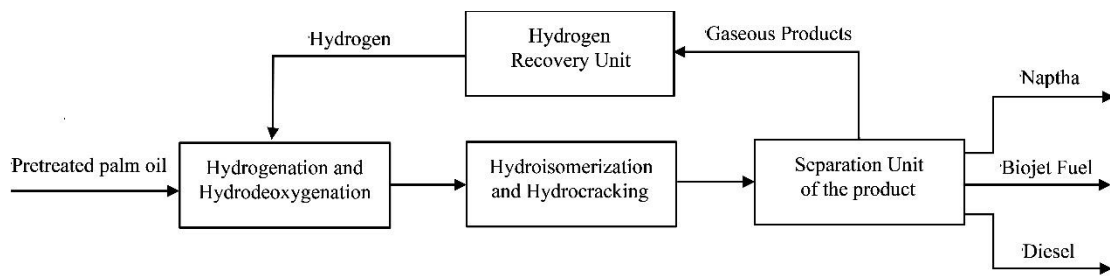


Figure 8 Block flow diagram of scenario 1

Scenario 2 (SAF production with hydrogen generation via biomass gasification):

In scenario 2, the process involves the integration of a catalytic deoxygenation plant with a hydrogen generation unit through biomass gasification. This gasification process transforms biomass into syngas at elevated temperatures, devoid of combustion, and under controlled conditions involving air, oxygen, and/or steam, as depicted in Figure 9.

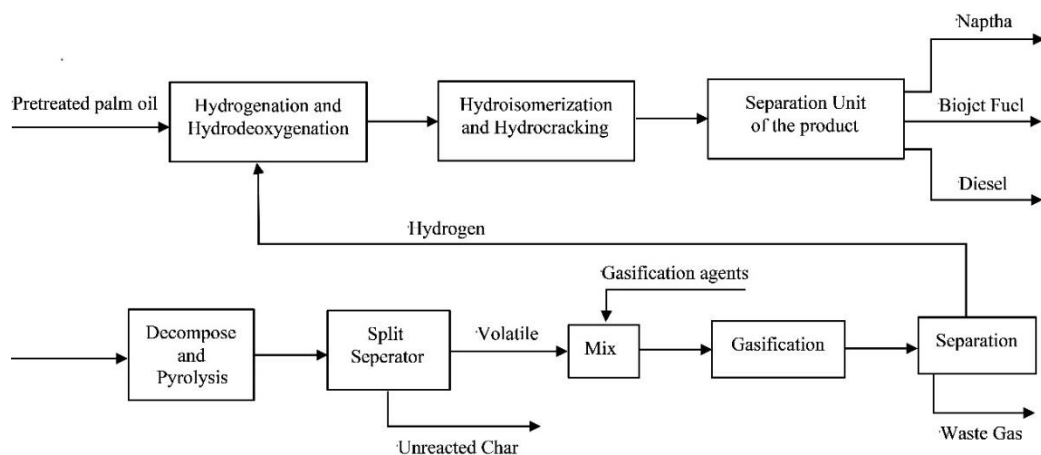


Figure 9 Block flow diagram of scenario 2

3.4 Process Simulation

The initial stage of the methodology involves the characteristics of the feedstock by vary based on the composition of the feedstock and the operational conditions of the process. The properties of the feedstock serve as inputs for the Aspen Plus modeling. Crude palm oil predominantly consists of the mono-unsaturated fatty acid known as oleic acid. The triglyceride containing oleic acid, referred to as triolein, is among the triglycerides included in Aspen Plus's database. Consequently, the

simulation employed triolein to model crude palm oil. The biomass input of the model is palm kernel shell with a low content of water, therefore, the drying step is not required. Biomass and ash are specified as non-conventional components. The proximate analysis and ultimate analysis inserted in Aspen Plus are detailed in Table 4.

Aspen Plus software was employed to model all the processes, enabling the computation of mass and energy balances within the system. Thermodynamic and transport properties can be estimated using either the equation of state (EoS) or activity coefficient methods. Nonetheless, the EoS approach offers an edge due to its capability to cover a wide range of temperatures and pressures, resulting in improved precision. Thus, the Aspen models employed the Soave-Redlich-Kwong (SRK), as it was considered apt for accurately replicating thermochemical processes.

3.5 Process Evaluation

The model obtained from Aspen Plus will be used for evaluating the process in terms of economics, energy, and environmental impact using Aspen Economic Analyzer as follows.

3.5.1 Profitability Index (PI)

The Profitability Index (PI) serves as a metric that determines the viability of investing in the process. The equation for calculating PI is shown as follows [26].

$$\text{Profitability Index (PI)} = \frac{\text{Present value of future cash flows}}{\text{Initial investment}} \quad (6)$$

3.5.2 Internal Rate of Return (IRR)

The internal rate of return (IRR) represents a discount rate at which the net present value (NPV) of all cash flows becomes zero. IRR serves as an indicator of the potential profitability of an investment by using the following equations [27], [28].

$$0 = \text{NPV} = \sum_{t=1}^T \frac{C_t}{(1 + \text{IRR})^t} - C_0 \quad (7)$$

3.5.3 Payback Period

The payback period represents the duration needed to recoup the initial investment cost. A shorter payback period indicates that the project is a more appealing investment option. The payback period can be calculated as follows [29].

$$\text{Payback Period} = \frac{\text{Cost of Investment}}{\text{Average Annual Cash Flow}} \quad (8)$$

3.5.4 Energy Utilization

To evaluate the process's energy utilization, the specific energy consumption equation (SEC) used to quantify the amount of energy used per unit of output or production in a given process. This work is used to calculate the energy required to produce 1 kg of biojet fuel. The specific energy consumption (SEC) can be calculated as follows [30].

$$\text{Specific Energy Consumption (SEC)} = \frac{\text{Energy consumption}}{\text{Amount of SAF produced}} \quad (9)$$

3.5.5 Environmental Impact

The environmental impact of the process is determined by calculating the amount of CO₂ emitted per quantity of biojet fuel produced as follows.

$$\text{CO}_2 \text{ emission} = \frac{\text{Amount of CO}_2 \text{ emission}}{\text{Amount of SAF produced}} \quad (10)$$

Chapter 4

Results and Discussion

This chapter presents the results and discussion of the study by dividing it into four sections: the validation of the simulation model, the results of the SAF production with hydrogen recovery via steam reforming (Scenario 1), the results of the SAF production with hydrogen generation via biomass gasification (Scenario 2), and the comparison results between process in terms of process performance, economic results, and the environmental impact.

4.1 Model Validation

4.1.1 Thermodynamic Model Validation

This research explores mixtures containing hydrocarbons, light gases (such as carbon dioxide and hydrogen), and other mildly polar non-ideal chemicals. The thermodynamic model chosen for this study is the Soave-Redlich-Kwong (SRK) property method, particularly suitable for high-temperature and high-pressure conditions found in hydrocarbon processing applications. To ensure accurate results in vapor-liquid equilibrium (VLE) or liquid-liquid equilibrium (LLE) calculations, the binary parameters from Aspen Physical Property System's built-in binary parameters (PRKBV) were utilized to describe the interactions between components. Additionally, the Data Regression System was employed to determine binary parameters using experimental phase equilibrium data, typically binary VLE data. The thermodynamic validation focused on the behavior of a mixture of hydrogen gas and hexadecane (C₁₆H₃₄), as these are key components in the process, and relevant data is available in the National Institute of Standards and Technology database (NIST) within Aspen Plus.

Figure 10 shows the assessment of the thermodynamic model. The experimental data sourced from the NIST database in Aspen tools was juxtaposed with the predictions derived from the thermodynamic model. The findings suggest that the SRK model effectively characterizes the hydrogen and hexadecane system.

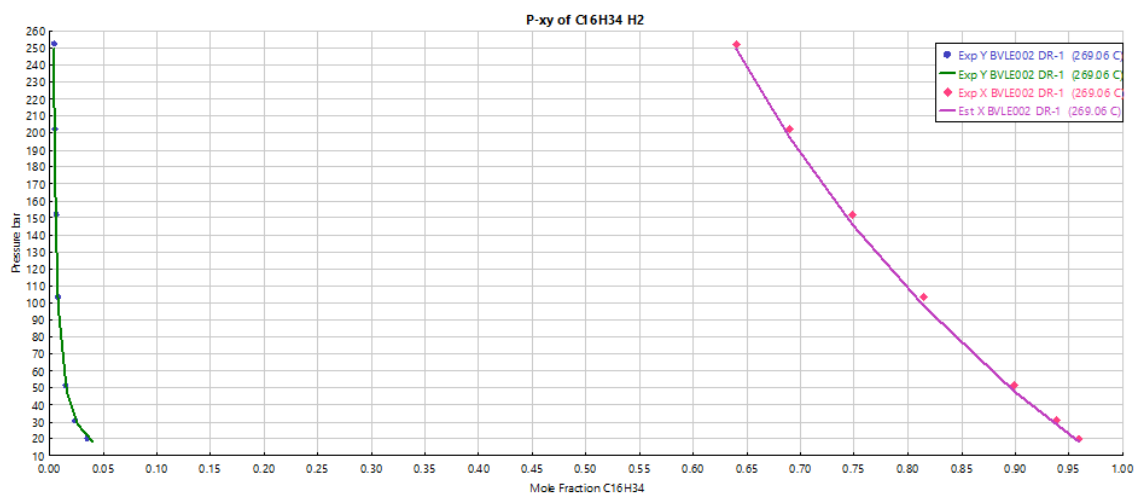


Figure 10 The behavior of hydrogen gas and hexadecane ($C_{16}H_{34}$) at 269 °C

4.1.2 SAF production with hydrogen recovery via steam reforming

Crude palm oil primarily consists of a mono-unsaturated fatty acid known as oleic acid. The specific triglyceride formed from oleic acid is referred to as triolein, and this compound is present in the Aspen Plus database. Consequently, in the simulation process, crude palm oil was represented using triolein, similar to the study taken by Zoé Béalu [17] in researching the SAF process using rapeseed oil, where triolein was utilized in the simulation. This choice is justified by the relatively similar triglyceride compositions of crude palm oil and rapeseed oil, as shown in Table 6. Table 6 shows that most common vegetable oils, such as palm oil and rapeseed have mostly oleic, linoleic and palmitic acid as triglycerides.

Table 6 Triglycerides composition of several vegetable oils [9]

Name	Structure	Typical composition, wt. %				
		Jatropha	Palm	Canola (Rapeseed)	Soybean	Sunflower
Capric	C10:0	0.0	0.0	0.6	0.0	0.0
Lauric	C12:0	0.0	0.0	0.0	0.0	0.0
Myristic	C14:0	0.0	2.5	0.1	0.0	0.0
Palmitic	C16:0	15.9	40.8	5.1	11.5	6.5
Palmitoleic	C16:1	0.9	0.0	0.0	0.0	0.2
Stearic	C18:0	6.9	3.6	2.1	4.0	5.8
Oleic	C18:1	41.1	45.2	57.9	24.5	27.0
Linoleic	C18:2	34.7	7.9	24.7	53.0	60.0
Linolenic	C18:3	0.3	0.0	7.9	7.0	0.2
Arachidic	C20:0	0.0	0.0	0.2	0.0	0.3
Eicosenoic	C21:1	0.2	0.0	1.0	0.0	0.0
Behenic	C22:0	0.0	0.0	0.2	0.0	0.0
Erucic	C22:1	0.0	0.0	0.2	0.0	0.0

A process flow diagram of the SAF production with hydrogen recovery via steam reforming (Scenario 1) is shown in Figure 11 derived from a study of process simulation by Zoé Béalu [16]. Crude palm oil at 10,000 kg/h feed rate was heated from 25 to 319 °C by E-101 and hydrogen at 283 kg/h feed rate at 267 °C and 40 bar were transferred to the hydrogenation reactor (R-101), where hydrogenation reactions were simulated. As for the hydrogenation modeling, no reactions kinetic have been identified so far. Consequently, a yield reactor was selected for the hydrogenation phase, and the reaction product yields are detailed in Appendix C. The output from the hydrogenation reactor (R-101) was separated into vapor and liquid phases in the flash drum (F-101) which operates at 173 °C, 1 bar. A section of the vapor phase was heated by E-103, and water was separated from the stream at the flash drum (F-102). The remaining vapor phase was directed to the separator (S-101) to eliminate CO and CO₂. Simultaneously, a section of the gas from separator (S-101), composed of hydrocarbons, was utilized to supply the steam reforming unit. Concurrently, a section of the liquid phase from the hydrogenation reactor (R-101) proceeded to the hydrocracking and isomerization reactor (R-102), which, like the hydrogenation reactor, was simulated using a yield reactor with detailed yield curves in Appendix D. Before entering the distillation column, the isomerized and hydrocracked products were mixed with gas from the hydrogenation process. This mixture was then directed to the first distillation column (D-101) to separate naphtha in the vapor phase from other hydrocarbons in the liquid phase. Subsequently, the remaining liquid-phase hydrocarbons were sent to the second distillation column (D-102) to produce the desired HEFA jet fuel and diesel.

In the hydrogen recovery section, a fraction of the residual gas from the separator (S-101) and the entire naphtha product from the distillation column (D-101) were employed in the hydrogen recovery process. This process involved routing the hydrocarbon and remaining gas product to a steam reformer reactor (R-103) operating at 760°C and 20 bar, followed by a water-gas-shift reactor (R-104) operating at 230°C and 10 bar to enhance hydrogen content and prevent carbon monoxide formation. The remaining water and condensed hydrocarbons were separated from the gas products in the flash drum (F-105) operating at 50°C and 10 bar. Subsequently, the gas

products underwent pressure swing adsorption (PSA) unit to capture the hydrogen. The recovered hydrogen was then reintroduced into the feed for the hydrogenation reactor (R-101) and the hydrocracking and isomerization reactor (R-102). The stream results of scenario 1 is shown in Appendix A. The equipment designed operating conditions of scenario 1 is shown in Appendix E.

Comparing the simulation result with the mass balance of the HEFA process from the study by Zoé Béalu [16] as shown in Table 7, no significant deviations were observed. This confirms the accuracy and validity of the scenario 1 simulation.

Table 7 Comparing the mass balance of the HEFA process between Zoé Béalu study [16] and Scenario 1

	Zoé Béalu [16]	Scenario 1
Feed		
Crude Palm Oil (kg/h)	10,000	10,000.00
Fresh Hydrogen (kg/h)	397	397.00
Recovered Hydrogen (kg/h)	397	397.00
Steam (kg/h)	5,252	5,252.00
Air (kg/h)	2,763	2,763.00
Product		
SAF (kg/h)	7,710	7,710.18
Byproduct		
Light Gas (kg/h)	83	83.01
Naphtha (kg/h)	486	486.33
Diesel (kg/h)	267	266.25
Reaction		
SAF Yield (%)	77.10	77.10

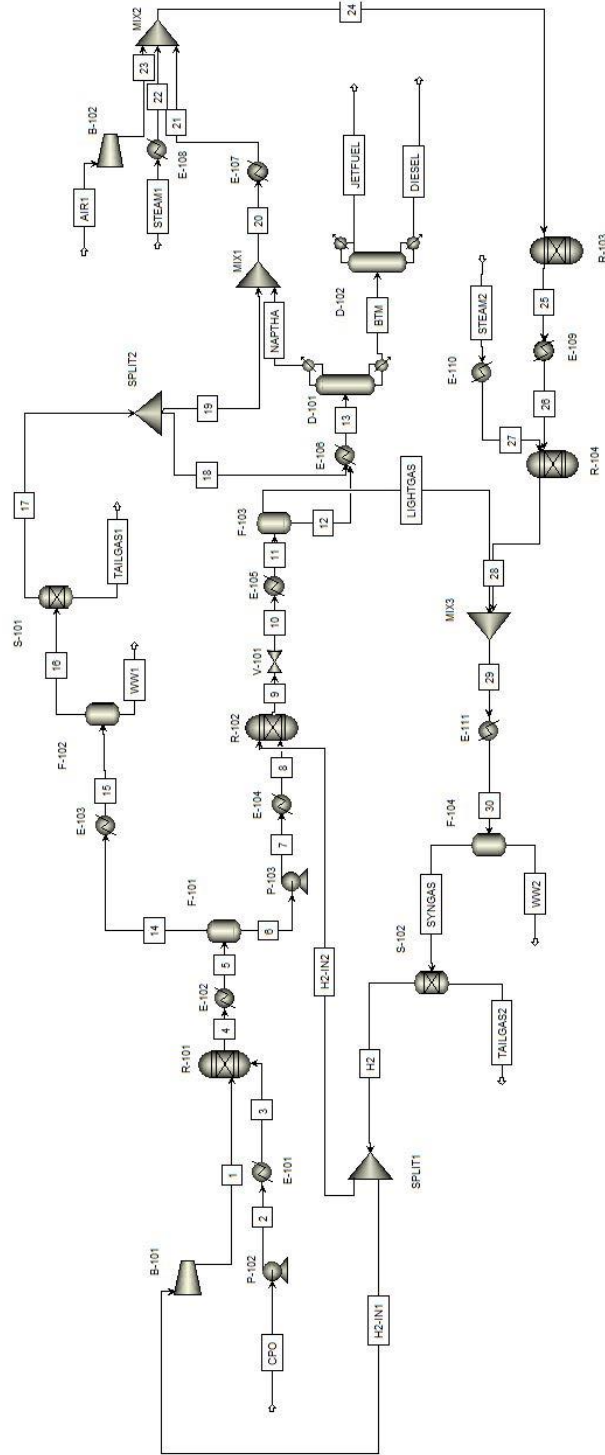


Figure 11 The designed process diagram results of scenario 1

4.1.3 SAF production with hydrogen generation via biomass gasification

A process flow diagram of the SAF production with hydrogen recovery via steam reforming (Scenario 2) is shown in Figure 12. Scenario 2 comprises two units: the SAF production unit and the biomass gasification unit. In the SAF production unit, the process is identical to that of Scenario 1, excluding the hydrogen recovery unit. This implies that all hydrogenated products are directly routed to the hydrocracking and isomerization reactor and subsequently sent to the first distillation column (D-101) for the separation of naphtha as a byproduct. The remaining hydrocarbon liquid is then forwarded to the second distillation column (D-102) to obtain jet fuel and diesel.

In the biomass gasification unit, the biomass stream, consisting of palm kernel shells and flowing at a rate of 14,550 kg/h, is directed into the R-201, a RYield reactor. This reactor is utilized to model the breakdown of the unconventional feed into its basic components (carbon, hydrogen, oxygen, sulfur, nitrogen, and ash). The yield distribution is specified based on the biomass ultimate analysis provided in Table 4. The decomposition of biomass in its chemical compounds was directly extended to the R-202, an RGibbs reactor conducting pyrolysis at a temperature of 700°C and a pressure of 1 bar. The resulting stream then proceeds into the splitter, where it is divided into two substreams: stream No. 14 containing the volatile component and the char part directed to stream CHAR. The volatile part in stream No. 14, upon being combined with steam as the gasifying agent, proceeds into the first gasifier reactor (R-203). The R-203 modeled the oxidation and reduction process, simulating the oxidation and reduction reactions in the gasifier. The R-201 reactors were simulated using the R-Plug model, which emulates ideal reactors operating at 700°C under atmospheric pressure. The actual temperature profile and dimensions of the reactor (with a reaction chamber of 0.25 m internal diameter and 2.3 m height) were specified. Additionally, the reactions involved in the gasification process and their respective kinetic parameters [19]. Finally, the product was directed to the pressure swing adsorption (PSA) unit for hydrogen capture. The hydrogen obtained from the biomass gasification unit was then directed into the feed for the hydrogenation reactor (R-101) and the

hydrocracking and isomerization reactor (R-102) to produce biojet fuel. The simulation result with the mass balance of scenario 2 is shown in Table 8. The stream results of scenario 1 is shown in Appendix B. The equipment designed operating conditions of scenario 1 is shown in Appendix F.

Table 8 The mass balance of scenario 2

Biomass Gasification Unit	Mass Flow (kg/h)
Feed	
Palm Kernel Shell	14,550.00
Steam	10,600.00
Product	
Green Hydrogen	397.88
HEFA Unit	Mass Flow (kg/h)
Feed	
Crude Palm Oil	10,000.00
Green Hydrogen	397.88
Product	
SAF	9,560.63
Byproduct	
Light Gas	103.34
Naphtha	454.75
Diesel	279.16

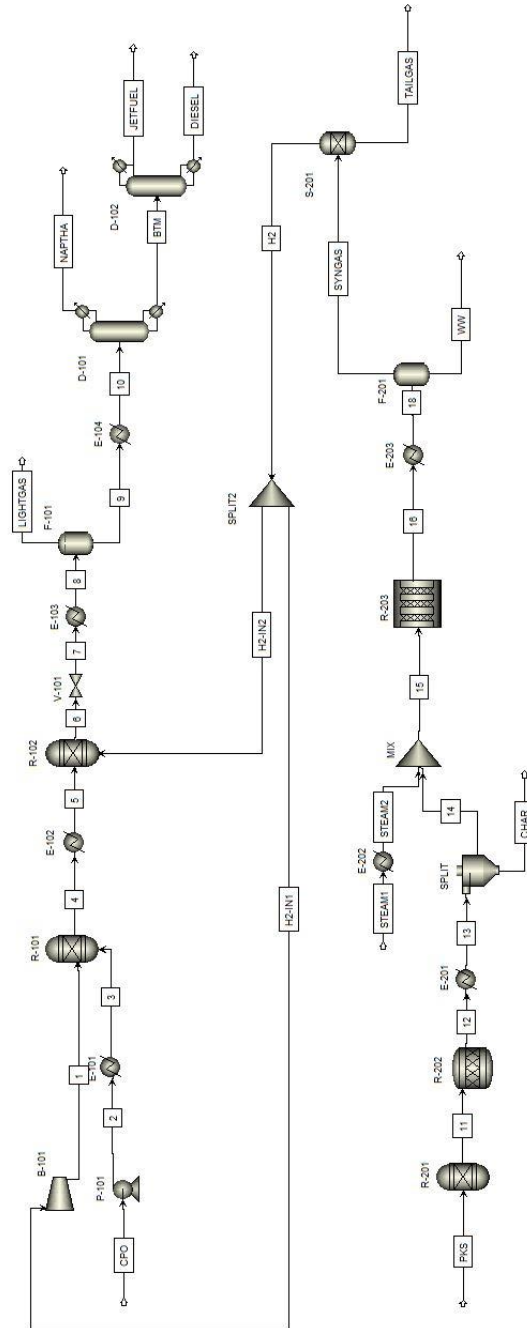


Figure 12 The designed process diagram results of scenario 2

Anyway, scenario 2 has been validated with experimental data of fluidized bed gasifier that utilized palm kernel shell as biomass from the literature of Khan et al [31] in terms of effect of gasification temperature and steam per biomass ratio. The results indicated a good agreement between the reported data and the values predicted by the model varied in terms of effect of gasification temperature.

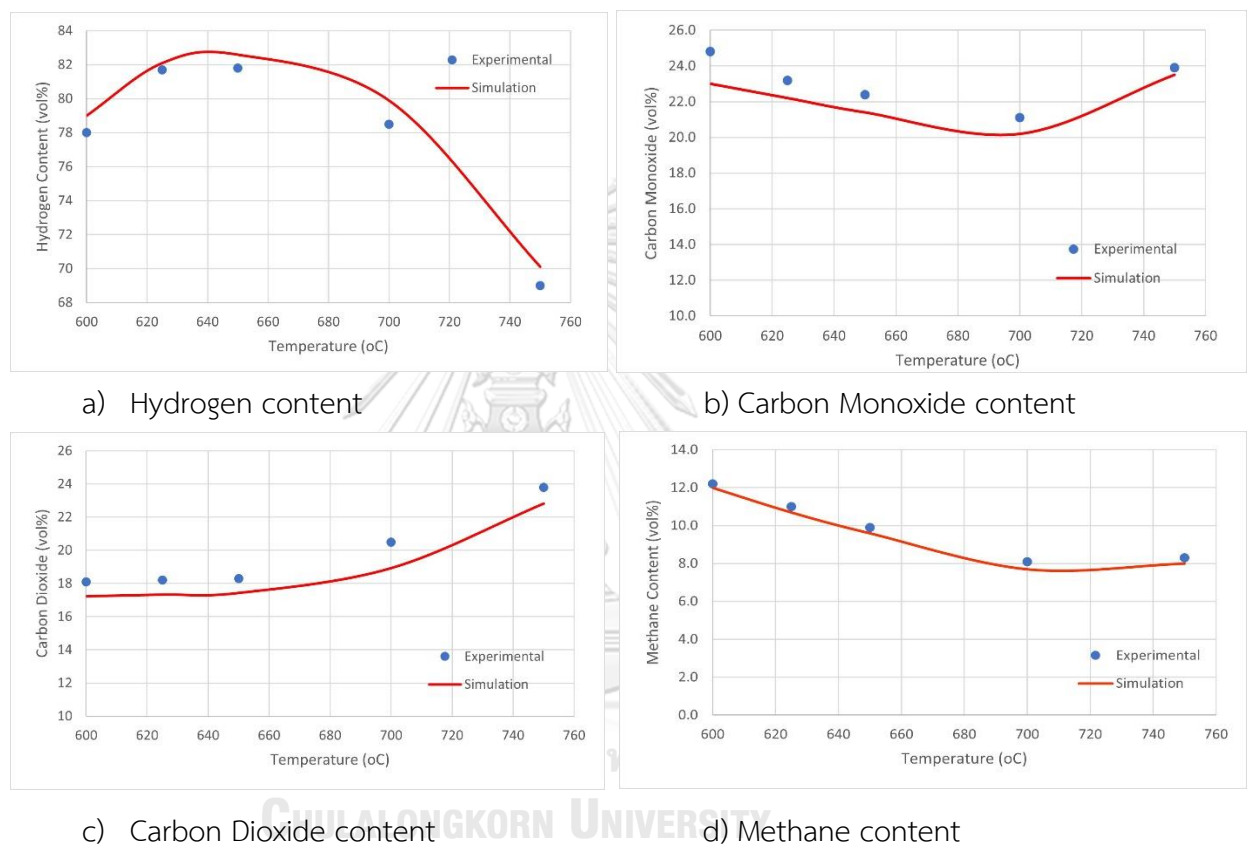


Figure 13 Effect of gasification temperature on syngas composition

Figure 13 shows the syngas product composition under specific conditions ($S/B = 0.7$ and $P_{op} = 1$ bar) at various temperatures ($T_{op} = 600^{\circ}\text{C}$, 625°C , 650°C , 700°C , and 750°C). A comparison between the experimental and simulated data is presented in Figure 13(a)-(d). The results indicate a close alignment between the model-predicted syngas concentrations and the experimental data, with root mean square error (RMSE) values of 0.99 for H_2 , 1.10 for CO , 1.07 for CO_2 , and 0.31 for CH_4 . At increasing temperatures, the H_2 content in the gas composition increases as the temperature rises from 600 to 700 $^{\circ}\text{C}$. Conversely, CO production decreases within this temperature range

but starts to increase after reaching 700 °C. This is attributed to the heightened occurrence of reactions, particularly the water gas shift reaction. The production of CO₂ is comparatively lower between 600 and 700 °C and begins to escalate beyond 700 °C.

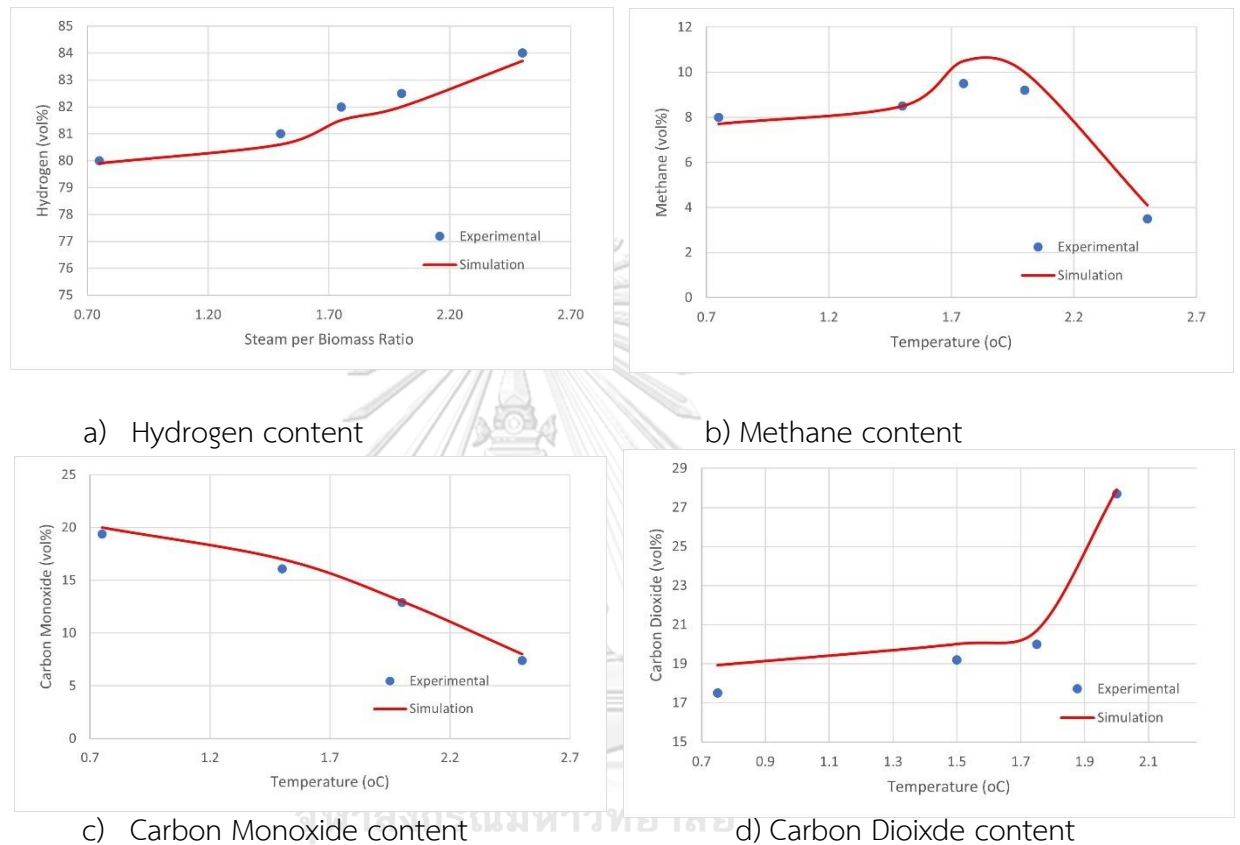


Figure 14 Effect of steam per biomass ratio on syngas composition

Figure 14 shows the syngas product composition under specific conditions $T_{op} = 800$ °C and $P_{op} = 1$ bar, at various ($S/B = 0.70, 1.5, 1.75,$ and 2). A comparison between the experimental and simulated data is presented in Figure 14(a)-(d). The results indicate a close alignment between the model-predicted syngas concentrations and the experimental data, with root mean square error (RMSE) values of 0.39 for H₂, 0.62 for CO, 0.89 for CO₂, and 0.65 for CH₄. Increasing S/B ratio results in an increase in H₂ production, rising from 80% to 84%. This increment, shown in Figure 14(a) demonstrates a notable 4% improvement in H₂ production. Concurrently, Figure 14(b)

shows a rise in methane production. Conversely, Figure 14(c) indicates a decrease in CO levels with an increased S/B ratio. This suggests that at lower S/B ratio, insufficient steam may be available to engage in biomass reactions, potentially limiting water-gas shift and steam reforming reactions. Therefore, an increased S/B ratio is likely to improve H₂ yield.

4.1.4 Process optimization of biomass gasification unit

Through this simulation, palm kernel shells can produce hydrogen at a rate of 27.33 g H₂/ kg palm kernel shell. Ng et al. [32] have similarly reported that the gasification of palm kernel shells achieves the highest hydrogen production, reaching 28.48 g H₂/ kg of palm kernel shell. Anyway, different gasification conditions can lead to variations in the composition and quantity of the produced gases, including hydrogen. This work explores the impact of operational parameters, specifically the gasifier temperature, and the ratio of steam to biomass on the composition of the resulting product gas. Utilizing a simulation model, the overall process performance is predicted, offering insights that can guide further optimization of the process.

According to the above sensitivity analysis to validate model, the syngas compositions exhibit sensitivity to variations in gasification temperature and steam per biomass ratio. Figure 13 and 14 highlight the ability to maximize the percentage composition of hydrogen in the syngas while minimizing the content of other components. In this study, the optimal operating conditions are determined to be a temperature set at 700°C and a steam per biomass ratio of 0.7. These conditions result in syngas with a desirable high hydrogen percentage and low concentrations of other components.

4.2 Comparison

4.2.1 Process Performance and Specific Energy Consumption

The process performance assessments for SAF production with hydrogen recovery via steam reforming (scenario 1) and SAF production with hydrogen generation via biomass gasification (scenario 2) are shown in Table 9.

Table 9 Process Performance comparison between scenario 1 and scenario 2

	Scenario 1	Scenario 2
Reaction		
SAF Yield (%)	77.10	95.60
SAF Production (kg SAF/h)	7,710.18	9,560.63
Energy utilization		
Total heating duty (kW)	16,149.80	37,848.1
Total cooling duty (kW)	10,698.70	29,556.4
SEC (kWh/ kg SAF)	3.48	7.05

In both scenario 1 and scenario 2, hydrogen and crude palm oil are supplied at the same flow rate according to Table 7 and Table 8. However, scenario 2 achieves a higher SAF yield compared to scenario 1.

In scenario 1, there is a separation of vapor and liquid phases in stream no.5, with the vapor phase in stream no.14 passing to the flash drum (F-101) and the liquid fraction going to stream no.6 for hydrocracking and isomerization and the result product is in stream no. 9 as shown stream results in Table 11.

In scenario 2 all the product from hydrogenation process in stream no.4 is heated in the heater (E-102) to convert it into a liquid phase. This liquid phase in stream no.5 is then directed to the hydrocracking and isomerization reactor to generate hydrocarbons and the result product is in stream no. 6 as shown in Table 12. The key point is that in scenario 2, not separating the stream into vapor and liquid phases allows for more reactant and hydrocarbon to be available for further reactions in the

hydrocracking and isomerization reactor. This, in turn, leads to a higher yield of SAF compared to scenario 1.

The key point is that in scenario 2, not separating the stream into vapor and liquid phases allows for more hydrocarbon to be available for further reactions in the hydrocracking and isomerization reactor. This, in turn, leads to a higher yield of sustainable aviation fuel (SAF) compared to scenario 1. The specific energy consumption results show that scenario 2 requires higher energy consumption per product compared to scenario 1 because scenario 2 requires more complex and varied processing steps, such as pyrolysis, and gas cleaning. These steps can introduce additional energy requirements.

4.2.2 Process Economic Comparison

In terms of process economics, the two processes are evaluated using Aspen Economic Analyzer.

Table 10 Total capital cost of the two scenarios

Parameter (Million US\$)	Scenario 1	Scenario 2
Equipment and Installation Cost	6.73	4.82
- Reactor	1.86	1.33
- Distillation Column	1.57	1.70
- Heat Exchangers	2.90	0.85
- Flash Drum	0.22	0.49
- Pump	0.07	0.46
Instrumentation and Control Cost	0.89	1.22
Piping Costs	0.53	0.82
Electrical Costs	0.82	0.77
Civil and Structural Costs	0.11	1.32
Total Capital Cost	9.08	8.95

Table 10 provides a summary of the capital costs for both scenarios. The capital costs for both scenarios are relatively similar, with Scenario 1 incorporating a hydrogen recovery unit and Scenario 2 featuring an additional biomass gasification unit. In Scenario 1, the most significant equipment cost is attributed to heat exchangers, primarily designed for the hydrogen recovery unit to withstand high operating temperatures and pressures. In contrast, for Scenario 2, the highest equipment cost is associated with distillation columns. These columns are arranged sequentially to facilitate the separation of the product into naphtha, jet fuel, and diesel.

Table 11 Total operating cost of the two scenarios

Parameter (Million US\$/Year)	Scenario 1	Scenario 2
Raw Material Costs	24.16	70.33
Utility Costs	1.89	1.58
Labor Costs	0.53	0.70
Maintenance Costs	0.13	0.13
Plant Overhead Costs	0.50	0.60
Other Direct/ Indirect Costs	1.63	2.11
Total Operating Cost	28.82	75.45

Table 11 presented the operating costs for both scenarios. Although the overall operating cost for scenario 2 is higher than scenario 1, the breakdown indicates that a significant portion of the operating expenses is attributable to raw materials. In scenario 2, the total raw materials include palm kernel shell, crude palm oil, and steam. For scenario 1 involves raw materials such as hydrogen, crude palm oil, and steam. The design of scenario 2 necessitates a substantial quantity of palm kernel shell for the hydrogen production process, contributing to its higher operating cost compared to scenario 1, where some hydrogen is generated through the steam reforming unit.

Based on the summarized results presented in Table 12, the assessment of jet fuel profitability from both process routes involved optimizing various parameters

including payback period, profitability index and internal rate of return. In term of economic factors, when the profitability index (PI) is above 1, it means both processes are making a profit. Furthermore, when we look at the internal rate of return (%IRR) and the payback period, scenario 2 has a higher %IRR and a shorter payback period. This suggests that investing in scenario 2 is more appealing than scenario 1.

Table 12 Process economics comparison between the two scenarios

	Scenario 1	Scenario 2
Total Capital Cost (Million US\$)	9.08	8.95
Total Operating Cost (Million US\$)	28.82	75.45
Total Raw Material Cost (Million US\$)	24.16	66.33
Total Product Sales (Million US\$)	38.90	109.15
Total Utility Cost (Million US\$)	0.89	1.58
Payback Period (Year)	4.54	2.79
Profitability Index	1.10	1.18
Internal Rate of Return	43.92	77.16

4.2.3 Environmental impact comparison

The total carbon dioxide emissions are divided into two main types including direct emissions come from sources and indirect emissions from the use of utilities. In term of environmental impact assessment, the total carbon dioxide emissions are used to compare between the two scenarios. The assessment of carbon dioxide emissions is represented in Table 13.

Table 13 Environmental impact comparison between scenario 1 and scenario 2

Parameter (kg CO ₂ /h)	Scenario 1	Scenario 2
Direct Emissions (from sources)	8,104.2	30,525.3
Indirect Emission (from utilities)	745.6	4,291.0
- Medium Pressure Stream	45.7	1,938.5
- High Pressure Stream	164.0	137.0
- Natural Gas	535.9	2,214.5
Total CO ₂ Emissions	8,849.8	34,816.3
Specific CO₂ Emissions	1.15	3.64

As per the assessment of environmental impact, the results indicate that scenario 2 exhibits greater carbon dioxide emissions in comparison to scenario 1. This discrepancy arises from the fact that scenario 2 utilizes more energy than scenario 1, and the quantity of energy consumed directly influences in utility usage. Anyway, this is also because the release of carbon dioxide from biomass gasification in scenario 2 is indeed associated with the combustion of carbon-containing compounds, including carbon in the form of char and ash.

Chapter 5

Conclusions

5.1 Conclusions

The comparative analysis of two scenarios for enhancing biojet fuel production processes reveals distinct advantages and challenges. Scenario 1, focused on hydrogen recovery via steam reforming, and Scenario 2, involving hydrogen generation via biomass gasification, present contrasting outcomes in terms of process performance, economic viability, and environmental impact.

Scenario 1, with its emphasis on hydrogen recovery, demonstrates a respectable SAF yield of 77.10%. However, the specific energy consumption (SEC) is relatively lower at 3.48 kWh/kg SAF, indicating a more straightforward and energy-efficient process. The economic evaluation reveals a payback period of 4.54 years, a profitability index of 1.10, and an internal rate of return (IRR) of 43.92%, making it a financially viable option. On the other hand, Scenario 2, integrating hydrogen generation via biomass gasification, achieves a significantly higher SAF yield of 95.60%. Despite a higher SEC of 7.05 kWh/kg SAF, the economic metrics present a compelling case, with a shorter payback period of 2.79 years, a higher profitability index of 1.18, and an impressive IRR of 77.16%. This scenario proves to be more economically attractive due to its enhanced SAF production efficiency. However, the environmental impact assessment highlights a trade-off. Scenario 2 incurs greater carbon dioxide emissions compared to Scenario 1. This disparity is primarily attributed to the increased energy demand and varied processing steps.

In summary, while Scenario 2 exhibits superior SAF production efficiency and economic feasibility, it comes at the cost of higher carbon dioxide emissions. The choice between the two scenarios should consider a balanced approach, considering environmental sustainability alongside economic and production efficiency factors. This comprehensive evaluation provides valuable insights for stakeholders in the biojet fuel production industry, contributing to informed decision-making for a sustainable and economically viable future.

Appendix A Stream results of Scenario 1 (Cont'd)

Stream no.	STEAM1	22	AIR1	23	24	25	26
Temperature (°C)	25	760	25	557	725	760	230
Pressure (bar)	1	20	1	20	20	20	10
Mass Vapor Fraction	0	1	1	1	1	1	1
Mass Flows (kg/h)	4,396.00	4,396.00	2,763.00	2,763.00	8,619.38	8,619.38	8,619.38
TRIOLEIN	0.00	0.00	0.00	0.00	0.00	0.00	0
H ₂	0.00	0.00	0.00	0.00	1.24	427.16	427.16
C ₃ H ₈	0.00	0.00	0.00	0.00	570.26	0.00	0.00
C ₄ H ₁₀	0.00	0.00	0.00	0.00	1.01	0.00	0.00
C ₅ H ₁₂	0.00	0.00	0.00	0.00	3.98	0.00	0.00
C ₆ H ₁₄	0.00	0.00	0.00	0.00	9.71	0.00	0.00
C ₇ H ₁₆	0.00	0.00	0.00	0.00	18.62	0.00	0.00
C ₈ H ₁₈	0.00	0.00	0.00	0.00	110.17	0.00	0.00
C ₉ H ₂₀	0.00	0.00	0.00	0.00	292.69	0.00	0.00
C ₁₀ H ₂₂	0.00	0.00	0.00	0.00	13.80	0.00	0.00
C ₁₁ H ₂₄	0.00	0.00	0.00	0.00	8.06	0.00	0.00
C ₁₂ H ₂₆	0.00	0.00	0.00	0.00	4.33	0.00	0.00
C ₁₃ H ₂₈	0.00	0.00	0.00	0.00	2.75	0.00	0.00
C ₁₄ H ₃₀	0.00	0.00	0.00	0.00	1.84	0.00	0.00
C ₁₅ H ₃₂	0.00	0.00	0.00	0.00	67.51	0.00	0.00
C ₁₆ H ₃₄	0.00	0.00	0.00	0.00	41.72	0.00	0.00
C ₁₇ H ₃₆	0.00	0.00	0.00	0.00	130.01	0.00	0.00
C ₁₈ H ₃₈	0.00	0.00	0.00	0.00	81.82	0.00	0.00
C ₁₉ H ₄₀	0.00	0.00	0.00	0.00	3.07	0.00	0.00
CO	0.00	0.00	0.00	0.00	48.97	1,454.65	1,454.65
CO ₂	0.00	0.00	0.00	0.00	48.82	1,992.58	1,992.58
H ₂ O	4,396.00	4,396.00	0.00	0.00	4,396.00	2,625.53	2,625.53
O ₂	0.00	0.00	643.55	643.55	643.55	0.00	0.00
N ₂	0.00	0.00	2,119.45	2,119.45	2,119.45	2,119.45	2,119.45

Appendix A Stream results of Scenario 1 (Cont'd)

Stream no.	STEAM2	27	28	29	30	SYNGAS
Temperature (°C)	25	230	230	231	50	50
Pressure (bar)	1	10	10	10	10	10
Mass Vapor Fraction	0	1	1	1	1	1
Mass Flows (kg/h)	856.00	856.00	9,475.38	9,558.39	9,558.39	6,864.92
TRIOLEIN	0.00	0.00	0.00	0.00	0.00	0.00
H ₂	0.00	0.00	501.91	502.53	502.53	502.53
C ₃ H ₈	0.00	0.00	0.00	0.00	0.00	0.00
C ₄ H ₁₀	0.00	0.00	0.00	8.30	8.30	8.30
C ₅ H ₁₂	0.00	0.00	0.00	8.30	8.30	8.30
C ₆ H ₁₄	0.00	0.00	0.00	8.30	8.30	8.30
C ₇ H ₁₆	0.00	0.00	0.00	8.30	8.30	8.30
C ₈ H ₁₈	0.00	0.00	0.00	49.18	49.18	49.18
C ₉ H ₂₀	0.00	0.00	0.00	0.00	0.00	0.00
C ₁₀ H ₂₂	0.00	0.00	0.00	0.00	0.00	0.00
C ₁₁ H ₂₄	0.00	0.00	0.00	0.00	0.00	0.00
C ₁₂ H ₂₆	0.00	0.00	0.00	0.00	0.00	0.00
C ₁₃ H ₂₈	0.00	0.00	0.00	0.00	0.00	0.00
C ₁₄ H ₃₀	0.00	0.00	0.00	0.00	0.00	0.00
C ₁₅ H ₃₂	0.00	0.00	0.00	0.00	0.00	0.00
C ₁₆ H ₃₄	0.00	0.00	0.00	0.00	0.00	0.00
C ₁₇ H ₃₆	0.00	0.00	0.00	0.00	0.00	0.00
C ₁₈ H ₃₈	0.00	0.00	0.00	0.00	0.00	0.00
C ₁₉ H ₄₀	0.00	0.00	0.00	0.00	0.00	0.00
CO	0.00	0.00	368.38	368.38	368.38	368.38
CO ₂	0.00	0.00	3,706.26	3,706.26	3,706.26	3,706.07
H ₂ O	856.00	856.00	2,779.35	2,779.35	2,779.35	86.11
O ₂	0.00	0.00	0.00	0.00	0.00	0.00
N ₂	0.00	0.00	2,119.45	2,119.45	2,119.45	2,119.45

Appendix A Stream results of Scenario 1 (Cont'd)

Stream no.	WW2	H2	TAILGAS2	H2-IN2
Temperature (°C)	50	50	50	50
Pressure (bar)	10	10	10	10
Mass Vapor Fraction	0	1	1	1
Mass Flows (kg/h)	6,864.92	397.00	6,467.92	114.00
TRIOLEIN	0.00	0.00	0.00	0.00
H ₂	502.53	397.00	105.53	114.00
C ₃ H ₈	0.00	0.00	0.00	0.00
C ₄ H ₁₀	8.30	0.00	8.30	0.00
C ₅ H ₁₂	8.30	0.00	8.30	0.00
C ₆ H ₁₄	8.30	0.00	8.30	0.00
C ₇ H ₁₆	8.30	0.00	8.30	0.00
C ₈ H ₁₈	49.18	0.00	49.18	0.00
C ₉ H ₂₀	0.00	0.00	0.00	0.00
C ₁₀ H ₂₂	0.00	0.00	0.00	0.00
C ₁₁ H ₂₄	0.00	0.00	0.00	0.00
C ₁₂ H ₂₆	0.00	0.00	0.00	0.00
C ₁₃ H ₂₈	0.00	0.00	0.00	0.00
C ₁₄ H ₃₀	0.00	0.00	0.00	0.00
C ₁₅ H ₃₂	0.00	0.00	0.00	0.00
C ₁₆ H ₃₄	0.00	0.00	0.00	0.00
C ₁₇ H ₃₆	0.00	0.00	0.00	0.00
C ₁₈ H ₃₈	0.00	0.00	0.00	0.00
C ₁₉ H ₄₀	0.00	0.00	0.00	0.00
CO	368.38	0.00	368.38	0.00
CO ₂	3,706.07	0.00	3,706.07	0.00
H ₂ O	86.11	0.00	86.11	0.00
O ₂	0.00	0.00	0.00	0.00
N ₂	2,119.45	0.00	2,119.45	0.00

Appendix B Stream results of scenario 2

Stream no.	PKS	11	12	13	14
Temperature (°C)	700	700	900	700	700
Pressure (bar)	1	1	10	1	1
Mass Solid Fraction	1	0.47	0.29	0.29	0
Mass Vapor Fraction	0	0.53	0	0.71	1
Mass Flows (kg/h)	14,550.00	14,550.00	14,550.00	14,550.00	10,394.10
BIOMASS	14,550.00	0.00	0.00	0.00	0.00
ASH	0.00	292.22	292.22	292.22	0.00
C	0.00	6,540.97	3,863.65	3,863.65	0.00
H ₂ O	0.00	1,022.96	3,806.22	3,806.22	3,806.22
S	0.00	2.71	2.71	2.71	2.71
CO	0.00	0.00	837.02	837.02	837.02
CO ₂	0.00	0.00	3,921.20	3,921.20	3,921.20
N ₂	0.00	64.94	64.94	64.94	64.94
O ₂	0.00	5,800.96	0.00	0.00	0.00
CH ₄	0.00	0.00	1,667.21	1,667.21	1,667.21
H ₂	0.00	825.24	94.80	94.80	94.80

Appendix B Stream results of scenario 2 (Cont'd)

Stream no.	CHAR	H2O	STEAM	15	16
Temperature (°C)	700	25	150	430	700
Pressure (bar)	1	1	1	1	1
Mass Solid Fraction	1	0	0	0	0
Mass Vapor Fraction	0	0	1	1	1
Mass Flows (kg/h)	4,115.87	10,600.00	10,600.00	20,994.10	20,994.10
BIOMASS	0.00	0.00	0.00	0.00	0.00
ASH	292.22	0.00	0.00	0.00	0.00
C	3,863.65	0.00	0.00	0.00	0.00
H ₂ O	0.00	10,600.00	10,600.00	14,406.22	13,177.55
S	0.00	0.00	0.00	2.71	2.71
CO	0.00	0.00	0.00	837.02	2,697.16
CO ₂	0.00	0.00	0.00	3,921.20	3,960.65
N ₂	0.00	0.00	0.00	64.94	64.94
O ₂	0.00	0.00	0.00	0.00	0.00
CH ₄	0.00	0.00	0.00	1,667.21	587.45
H ₂	0.00	0.00	0.00	94.80	503.64

Appendix B Stream results of scenario 2 (Cont'd)

Stream no.	17	SYNGAS	WW	H2	TAILGAS
Temperature (°C)	1	1	1	1	1
Pressure (bar)	21	21	21	15.7	15.7
Mass Solid Fraction	0	0	0	0	0
Mass Vapor Fraction	0.37	1	0	1	1
Mass Flows (kg/h)	20,994.10	7,815.35	13,178.80	397.88	7,417.47
BIOMASS	0.00	0.00	0.00	0.00	0.00
ASH	0.00	0.00	0.00	0.00	0.00
C	0.00	0.00	0.00	0.00	0.00
H ₂ O	13,177.55	2.43	13,175.12	0.00	0.00
S	2.71	0.00	2.71	0.00	0.00
CO	2,697.16	2,697.15	0.00	0.00	2,697.16
CO ₂	3,960.65	3,959.71	0.94	0.00	3,959.71
N ₂	64.94	64.94	0.00	0.00	64.94
O ₂	0.00	0.00	0.00	0.00	0.00
CH ₄	587.44	587.44	0.01	0.00	587.44
H ₂	503.64	503.64	0.00	397.88	106.46

Appendix C Yield curve of experimental studies for the hydrogenation reactor [16]

Reaction Products	Yield curve (wt%)
C_4H_{10}	0.01
C_5H_{12}	0.04
C_6H_{14}	0.10
C_7H_{16}	0.20
C_8H_{18}	0.21
C_9H_{20}	0.28
$C_{10}H_{22}$	0.25
$C_{11}H_{24}$	0.18
$C_{12}H_{26}$	0.13
$C_{13}H_{28}$	0.12
$C_{14}H_{30}$	0.12
$C_{15}H_{32}$	6.85
$C_{16}H_{34}$	6.63
$C_{17}H_{36}$	33.98
$C_{18}H_{38}$	33.69
$C_{19}H_{40}$	2.02
C_3H_8	5.6
CO	1.06
CO ₂	1.06
H ₂ O	7.5

Appendix D Yield curve of experimental studies for the hydrogenation reactor [16]

Reaction Products	Yield curve (wt%)
C_4H_{10}	0.1
C_5H_{12}	0.1
C_6H_{14}	0.1
C_7H_{16}	0.1
C_8H_{18}	1.7
C_9H_{20}	8.9
$C_{10}H_{22}$	14.3
$C_{11}H_{24}$	16.6
$C_{12}H_{26}$	16.6
$C_{13}H_{28}$	13.8
$C_{14}H_{30}$	12.9
$C_{15}H_{32}$	7.3
$C_{16}H_{34}$	5.4
$C_{17}H_{36}$	2.1
$C_{18}H_{38}$	0.3

Appendix E Equipment designed operating conditions of scenario 1.

Unit	Equipment	Operating Conditions	Design Comments
B-101	Pump	- Outlet Pressure = 40 bar	Designed based on Zoe Bealu [16]
P-102	Pump	- Outlet Pressure = 40 bar	
E-101	Heater	- Outlet Temperature = 319 °C - Pressure Drop = 40 bar	
R-101	RYield	- Temperature = 350 °C - Pressure = 40 bar	
E-102	Heater	- Outlet Temperature = 250 °C - Pressure Drop = 10 bar	
F-101	Flash	- Temperature = 173 °C - Pressure = 1 bar	
P-103	Pump	- Outlet Pressure = 70 bar	
E-104	Heater	- Outlet Temperature = 329 °C - Pressure Drop = 70 bar	
R-102	RYield	- Temperature = 362 °C - Pressure = 70 bar	
V-101	Valve	- Outlet Pressure = 15 bar	
E-105	Heater	- Outlet Temperature = 15 °C - Pressure Drop = 15 bar	
F-103	Flash	- Temperature = 344 °C - Pressure = 15 bar	
E-106	Heater	- Outlet Temperature = 130 °C - Pressure Drop = 1 bar	
D-101	Radfrac	- Reflux Ratio = 0.60 - Distillate Rate = 6.29 kmol/h	
D-102	Radfrac	- Reflux Ratio = 0.70 - Distillate Rate = 45.62 kmol/h	

E-103	Heater	- Outlet Temperature = 38 °C - Pressure Drop = 15.7 bar	Designed based on Zoe Bealu [16]
Unit	Equipment	Operating Conditions	Design Comments
F-102	Flash	- Temperature = 38 °C - Pressure = 15.7 bar	Designed based on Zoe Bealu [16]
S-101	Separator	Tail Gas Split Fraction - CO split fraction = 0.55 - CO ₂ split fraction = 0.55	
E-107	Heater	- Outlet Temperature = 760 °C - Pressure Drop = 20 bar	
B-102	Pump	- Outlet Pressure = 20 bar	
E-108	Heater	- Outlet Temperature = 760 °C - Pressure Drop = 20 bar	
R-103	RGibbs	- Temperature = 760 °C - Pressure = 20 bar	
E-109	Heater	- Outlet Temperature = 230 °C - Pressure Drop = 10 bar	
R-104	RGibbs	- Temperature = 230 °C - Pressure = 10 bar	
E-111	Heater	- Outlet Temperature = 50 °C - Pressure Drop = 10 bar	
F-104	Flash	- Outlet Temperature = 50 °C - Pressure Drop = 10 bar	
S-102	Separator	H ₂ Split Fraction - H ₂ split fraction = 0.74	

Appendix F Equipment designed operating conditions of scenario 2.

Unit	Equipment	Operating Conditions	Design Comments
B-101	Pump	- Outlet Pressure = 40 bar	Designed based on Zoe Bealu [16]
P-102	Pump	- Outlet Pressure = 40 bar	
E-101	Heater	- Outlet Temperature = 319 °C - Pressure Drop = 40 bar	
R-101	RYield	- Temperature = 350 °C - Pressure = 40 bar	
E-102	Heater	- Outlet Temperature = 329 °C - Pressure Drop = 70 bar	
R-102	RYield	- Temperature = 362 °C - Pressure = 70 bar	
V-101	Valve	- Outlet Pressure = 15 bar	
E-103	Heater	- Outlet Temperature = 15 °C - Pressure Drop = 15 bar	
F-101	Flash	- Temperature = 344 °C - Pressure = 15 bar	
E-104	Heater	- Outlet Temperature = 130 °C - Pressure Drop = 1 bar	
D-101	Radfrac	- Reflux Ratio = 0.36 - Distillate Rate = 4.79 kmol/h	From Design Spec
D-102	Radfrac	- Reflux Ratio = 0.70 - Distillate Rate = 45.62 kmol/h	
R-201	RYield	- Temperature = 700 °C - Pressure = 1 bar	

R-202	RGibbs	- Temperature = 900 °C - Pressure = 1 bar	Designed based on Gamero et al. [19]
E-201	Heater	- Outlet Temperature = 700 °C - Pressure Drop = 1 bar	
E-202 SPLIT	Heater Ssplit	- Outlet Temperature = 150 °C - Pressure Drop = 1 bar CHAR Stream Split Fraction - CISOLID stream =1 - NC stream =1	
R-203	RPlug	- Temperature = 700 °C - Pressure = 1 bar	Designed based on Gamero et al. [19]
		- Diameter = 0.25 m - Length = 2.3 m	From Calculation based on Khan et al. [32]
E-203	Heater	- Outlet Temperature = 1 °C - Pressure Drop = 21 bar	From Sensitivity Analysis
F-201	Flash	- Temperature = 1 °C - Pressure = 21 bar	
S-201	Separator	H ₂ Split Fraction - H ₂ split fraction =0.74	

REFERENCES

1. Umar M, Ji X, Kirikkaleli D, Alola AA. The imperativeness of environmental quality in the United States transportation sector amidst biomass-fossil energy consumption and growth. *Journal of Cleaner Production*. 2021;285:124863.
2. Hileman J, Stratton R. Alternative jet fuel feasibility. *Transport Policy*. 2014;34:52-62.
3. Lewis KC. Commercial aviation alternative fuels initiative. 2010.
4. Wang W-C, Tao L. Bio-jet fuel conversion technologies. *Renewable and Sustainable Energy Reviews*. 2016;53:801-22.
5. Yang J, Xin Z, Corscadden K, Niu H. An overview on performance characteristics of bio-jet fuels. *Fuel*. 2019;237:916-36.
6. Gutiérrez-Antonio C, Gómez-Castro FI, de Lira-Flores JA, Hernández S. A review on the production processes of renewable jet fuel. *Renewable and Sustainable Energy Reviews*. 2017;79:709-29.
7. Khan S, Lup ANK, Qureshi KM, Abnisa F, Daud WMAW, Patah MFA. A review on deoxygenation of triglycerides for jet fuel range hydrocarbons. *Journal of Analytical and Applied Pyrolysis*. 2019;140:1-24.
8. Plazas-González M, Guerrero-Fajardo CA, Sodr e JR. Modelling and simulation of hydrotreating of palm oil components to obtain green diesel. *Journal of Cleaner Production*. 2018;184:301-8.
9. Sotelo-Boy as R, Trejo-Z arraga F, Hern andez-Loyo F. Hydroconversion of triglycerides into green liquid fuels. *Hydrogenation*. 2012;338:338.
10. Vincent C, Claire C, Martina Kh. *Overview and Essentials of Biomass Gasification Technologies and Their Catalytic Cleaning Methods*. 2016.
11. Kalinci Y, Hepbasli A, Dincer I. Biomass-based hydrogen production: a review and analysis. *International journal of hydrogen energy*. 2009;34(21):8799-817.

12. Cabuk B, Duman G, Yanik J, Olgun H. Effect of fuel blend composition on hydrogen yield in co-gasification of coal and non-woody biomass. *International Journal of hydrogen energy*. 2020;45(5):3435-43.
13. Deva R, Ja M, Ma V. A Study approach of STEM for Biomass material for assessment of Gasification Process.
14. Parparita E, Uddin MA, Watanabe T, Kato Y, Yanik J, Vasile C. Gas production by steam gasification of polypropylene/biomass waste composites in a dual-bed reactor. *Journal of Material Cycles and Waste Management*. 2015;17:756-68.
15. Gong S, Shinozaki A, Shi M, Qian EW. Hydrotreating of jatropha oil over alumina based catalysts. *Energy & Fuels*. 2012;26(4):2394-9.
16. Béalu Z. Process Simulation and Optimization of Alternative Liquid Fuels Production A techno-economic assessment of the production of HEFA Jet Fuel: University of Kaiserslautern; 2017.
17. Lang A, Elhaj HFA. THE WORLDWIDE PRODUCTION OF BIO-JET FUELS.
18. Pranolo SH, Waluyo J, Putro FA, Adnan MA, Kibria MG. Gasification process of palm kernel shell to fuel gas: pilot-scale experiment and life cycle analysis. *International Journal of Hydrogen Energy*. 2023;48(7):2835-48.
19. Puig-Gamero M, Pio D, Tarelho L, Sánchez P, Sanchez-Silva L. Simulation of biomass gasification in bubbling fluidized bed reactor using aspen plus®. *Energy Conversion and Management*. 2021;235:113981.
20. Champion WM, Cooper CD, Mackie KR, Cairney P. Development of a chemical kinetic model for a biosolids fluidized-bed gasifier and the effects of operating parameters on syngas quality. *Journal of the Air & Waste Management Association*. 2014;64(2):160-74.
21. Gonzalez AM, Lora EES, Palacio JCE, del Olmo OAA. Hydrogen production from oil sludge gasification/biomass mixtures and potential use in hydrotreatment processes. *International Journal of Hydrogen Energy*. 2018;43(16):7808-22.
22. Zaccara A, Petrucciani A, Matino I, Branca TA, Dettori S, Iannino V, et al. Renewable hydrogen production processes for the off-gas valorization in integrated steelworks through hydrogen intensified methane and methanol syntheses. *Metals*. 2020;10(11):1535.

23. MATSUI I, KUNII D, FURUSAWA T. STUDY OF FLUIDIZED BED STEAM GASIFICATION OF CHAR BY THERMO GRAVIMETRIC ALLY OBTAINED KINETICS. Journal of chemical engineering of Japan. 1985;18(2):105-13.
24. Hsu K-H, Wang W-C, Liu Y-C. Experimental studies and techno-economic analysis of hydro-processed renewable diesel production in Taiwan. Energy. 2018;164:99-111.
25. Reniers G, Talarico L, Paltrinieri N. Cost-benefit analysis of safety measures. Dynamic risk analysis in the chemical and petroleum industry: Elsevier; 2016. p. 195-205.
26. Team C. Profitability Index: CFI; 2023 [Available from: <https://corporatefinanceinstitute.com/resources/accounting/profitability-index/>]
27. Tamplin T. How to Calculate IRR | IRR Formula 2023 [Available from: <https://www.financestrategists.com/wealth-management/accounting-ratios/irr/irr-formula/>].
28. IRR and NPV: Demystified: Gray Capital LLC; 2023 [Available from: <https://www.graycapitalllc.com/irr-and-npv-demystified/>].
29. Kagan J. Payback Period Explained, With the Formula and How to Calculate It 2023 [Available from: <https://www.investopedia.com/terms/p/paybackperiod.asp>].
30. Lawrence A, Thollander P, Andrei M, Karlsson M. Specific energy consumption/use (SEC) in energy management for improving energy efficiency in industry: Meaning, usage and differences. Energies. 2019;12(2):247.
31. Khan Z, Yusup S, Ahmad MM, Chin BLF. Hydrogen production from palm kernel shell via integrated catalytic adsorption (ICA) steam gasification. Energy Conversion and Management. 2014;87:1224-30.
32. Kotowicz J, Sobolewski A, Iluk T. Energetic analysis of a system integrated with biomass gasification. Energy. 2013;52:265-78.

VITA

NAME Praeva Pongsripipat

DATE OF BIRTH 17 December 1998

PLACE OF BIRTH Bangkok, Thailand

INSTITUTIONS ATTENDED B.Eng. Chemical Engineering, Srinakharinwirot University
M.Eng. Chemical Engineering, Chulalongkorn University

HOME ADDRESS 100 Ramintra 13, Ramintra Road, Anusawari, Bang khen,
Bangkok

